5-2022

Investigation of a Simultaneaous Direct and Indirect Contact Dehumidifier Using Parallel Strings for HDH Desalination

Josue Perez Perez
The University of Texas Rio Grande Valley

INVESTIGATION OF A SIMULTANEAOUS DIRECT AND INDIRECT CONTACT DEHUMIDIFIER USING PARALLEL STRINGS FOR HDH DESALINATION

A Thesis

by

JOSUE PEREZ PEREZ

Submitted in Partial Fulfillment of the

Requirements for the Degree of

MASTER OF SCIENCE IN ENGINEERING

Major Subject: Mechanical Engineering

The University of Texas Rio Grande Valley

May 2022

INVESTIGATION OF A SIMULTANEAOUS DIRECT AND INDIRECT CONTACT DEHUMIDIFIER USING PARALLEL STRINGS FOR HDH DESALINATION

A Thesis
by
JOSUE PEREZ PEREZ

COMMITTEE MEMBERS

Dr. Yingchen Yang
Chair of Committee

Dr. Javier Ortega
Committee Member

Dr. Maysam Pournik
Committee Member

May 2022

ABSTRACT

Perez Perez, Josue, Investigation of a simultaneous direct and indirect contact dehumidifier using parallel strings for HDH desalination. Master of Science in Engineering (MSE), May, 2022, 75 pp., 4 tables, 36 figures, references, 73 titles.

Freshwater is a limited and precious resource. Currently, half a billion people in the world face sever water scarcity all year round. Humidification dehumidification (HDH) systems have received special attention among the variety of small-scale desalination technologies due to its potential to create affordable and sustainable seawater desalination, especially when combined with natural power sources such as waves, wind, and solar rays. Improvements in the development of HDH desalination systems have been achieved in recent years. Nonetheless, the improvements that have received most attention focus on solar heaters and humidifiers. Dehumidification systems have often been adapted from air conditioning condensation systems rather than developed specifically for HDH applications.

This study focuses on the experimental design, testing, and analysis of a simultaneous direct and indirect contact dehumidifier using a bundle of parallel strings for HDH desalination applications. The use of cylindrical surfaces parallel to the flow to improve heat transfer has been widely investigated and utilized for indirect contact cooling (i.e shell and tube heat exchangers). However, there are limited investigations on the use of parallel strings to enhance direct-contact heat and mass transfer. Furthermore, the use of a bundle of parallel strings for the application of ocean-based humidification dehumidification (HDH) desalination has not been studied before.

Ocean-based systems introduce another level of complexity due to its remote location and weather exposure that requires the application of simple and robust designs. For this reason, the design under study is intended for applications which have no electric or electronic components, hence, improving its simplicity and costs by removing energy-requiring components (i.e. pumps, nozzles, sprays, etc). The dehumidifier under study solely relies on the use of highly efficient geometries introduced by the parallel strings to induce direct-contact heat and mass transfer and the ocean thermal energy for indirect-contact cooling. The application of the current dehumidifier is mainly centered on ocean-based HDH desalination technology; however, the general design concept could be implemented in other designs in which cooling, and dehumidification is desired for affordable and practical applications.

DEDICATION

I want to dedicate this work to God, without Him, nothing would've been possible. And to my wife, Martha, for her constant support, patience, and sincere love throughout this journey. Also, to my beloved daughters Marisol, Valeria, and Natalia, who are my source of motivation every day. And lastly, to my family, my parents, brothers, and sister, whose example and words of encouragement built a strong foundation for my success.

ACKNOWLEDGMENTS

I would like to give my most sincere gratitude to Dr. Yingchen Yang, whom without his guidance and support, this project wouldn't have been accomplished. His ability to help students on academic and personal issues is beyond imagination. I consider it a privilege to have worked under his supervision and will always cherish the moments I spent on the laboratory.

I would like to thank Dr. Javier Ortega and Dr. Maysam Pournik for their academic and moral support throughout my thesis project. Also, Dr. Crown and Dr. Choutapalli for their input and advice, and Alejandro Corona for working alongside with me on the lab. A special thanks to Antonio Suarez for being always available and willing to patiently help with the equipment in the machine shop and for his input on the machining of parts.

TABLE OF CONTENTS

Page

LIST OF TABLES

Page

LIST OF FIGURES

Page

CHAPTER I

INTRODUCTION

1.1 Motivation

Freshwater is a limited and precious resource. Currently, half a billion people in the world face sever water scarcity all year round [1]. Recent studies project water scarcity to increase and affect a great percentage of the world population causing many social and environmental concerns [2]. With this precious natural resource decreasing and human population increasing, the importance of finding efficient ways of obtaining fresh water has never been higher.

Research efforts have considered different solutions for freshwater production such as water treatment technologies, desalination, filtration and nanofiltration [3,4], thermal distillation, moisture harvesting, and fog collection [5,6]. Having over 97% of the total water of the world on the oceans, sea-water desalination is a promising technology for freshwater production [7]. Additionally, over 40% of the global population lives within 100 km of the coast [8], making seawater desalination an effective alternative to address water scarcity in coastal regions. Many desalination technologies have been proposed and studied in recent years. Reverse osmosis and multi-stage flash distillation are currently the most widely used method for large-scale (> 100 m^3/day) desalination [9]. The combination of these technologies with renewable sources of energy has been widely studied for a more environmentally friendly option and to reduce the cost

of operation [10]. On the other hand, small-scale desalination technologies (< 100 m^3/day) are very diverse. Small-scale desalination technologies have been mostly studied to meet the needs of rural areas, islands, and remote homes [11]. Among the most common technologies for small scale water desalination are Humidification-Dehumidification (HDH) desalination, solar stills [12], and direct moisture and fog water harvesting [5,6].

1.2 Humidification-Dehumidification desalination

The HDH technology is inspired by the natural hydrologic cycle as shown in Figure 1. Water naturally evaporates due to the heat of the sun forming clouds, and is later released in the form of freshwater rain. Similar to the rain cycle, a man-made HDH system circulates air

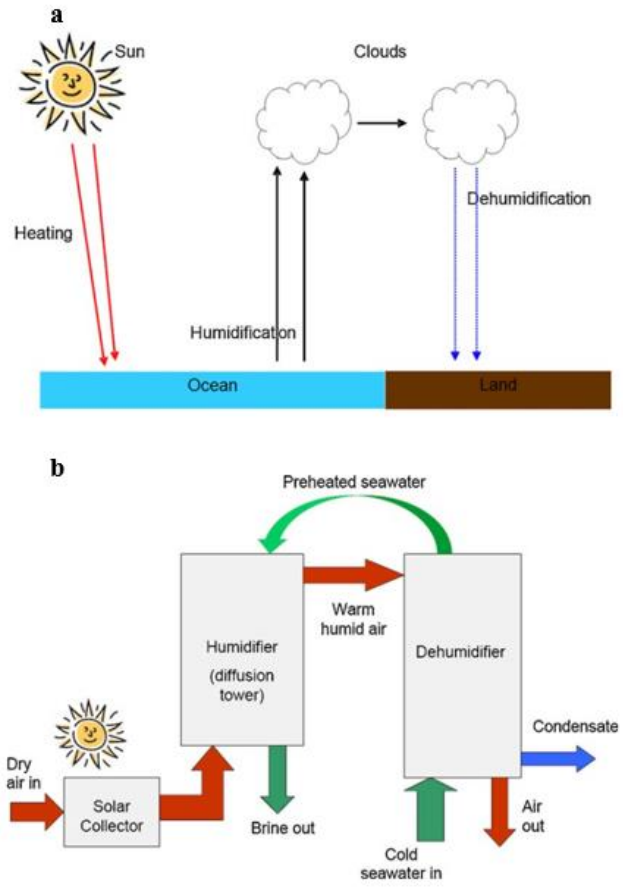

Figure 1: Solar humidification dehumidification process a) hydrologic cycle naturally occurring b) simple diagram of a man-made HDH system.

through series of components with thermodynamic and psychrometric changes that allow the air to mix with water vapor in a high temperature state (humidification), and then release the water at lower temperatures (dehumidification) to collect the condensate freshwater. HDH desalination is different from conventional distillation and solar stills systems mainly because of two factors: 1) HDH desalination required a forced gas flow that is circulated through a system and forced to absorb and release water molecules to produce the freshwater. 2) HDH systems generally operate under lower temperatures below the boiling temperature of water. The HDH desalination technology has received special attention among the variety of small-scale desalination techniques due to its potential to create affordable and sustainable seawater desalination, especially when combined with natural power sources such as waves, wind, and solar rays [13-15]. Many research activities have proven the HDH technology to be an inexpensive and reliable desalination approach [16].

HDH systems can be classified by 2 broad categories. The first classification is the type of energy used such as geothermal, thermal, solar, or hybrid systems. Using renewable energy sources is the key characteristic of the HDH system to lower the cost of freshwater production for a more affordable and sustainable desalination system. The second classification is based on the type of cycle. There are three types of cycles, closed-air open-water (CAOW), open-air closed-water (OACW), and open-air open-water (OAOW). As the name implies, a CWOA cycle is one in which the air is heated, humidified and dehumidified and let out in an open cycle. By contrast, in a closed-air cycle the air is circulated in a closed loop between the humidifier and the dehumidifier. The two cycles are illustrated in Figure 2. Open-air, open-water cycle is formed when the connection in the air stream between the humidifier and the dehumidifier is broken since the air stream makes a single pass through the system.

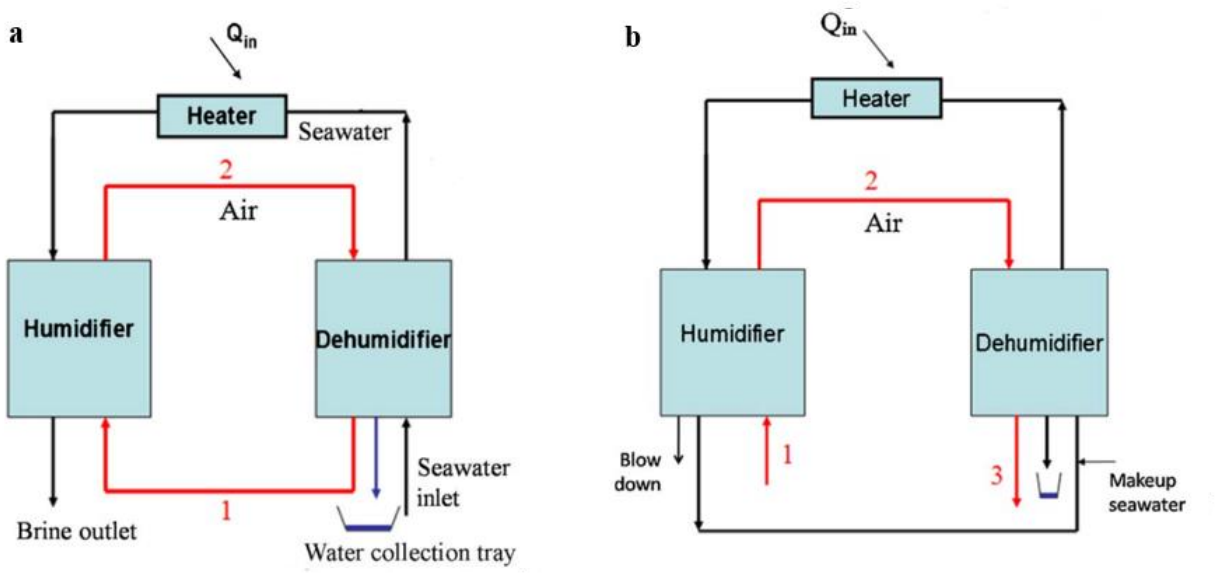

Figure 2: Diagram of the most investigated humidification dehumidification configurations. a) Closed-air open-water process. b) Open-air closed water process.

Other modifications that have been studied in the past are on the type of heating used on the system. A modified approach to the CAOW cycle shown in Figure 2a would be with the heater on the air side of the cycle as opposed to using a water heater. The performance of the system depends greatly on whether the air or water is heated. Among a large variety of solar HDH systems being explored so far, the most energy-efficient one is a multi-effect closed-air open-water system [17].

HDH desalination systems can be land-based or ocean-based. Nearly all research and documented literature has focus on the study of land-based systems due to its easy construction and testing and low operation and maintenance costs [13, 18]. For these reasons, research and invention disclosures on ocean based HDH desalination systems is very limited [18-22]. The advantage of ocean-based HDH desalination systems lies on utilizing the ocean energy (i.e., waves and ocean thermal), minimizing pre-treatment stages for a brine-free process and

minimizing brine-related maintenance costs [23]. Energy consumption of all types of desalination technologies is related to critical issues associated with environmental impact and the overall cost of operation. Ocean-based HDH desalination has the potential to lower such costs by employing a combination of multiple renewable energies for direct (without converting to electricity) or indirect (converting into electricity) use. A schematic of a completely nature-powered ocean-based HDH system is shown in Figure 3.

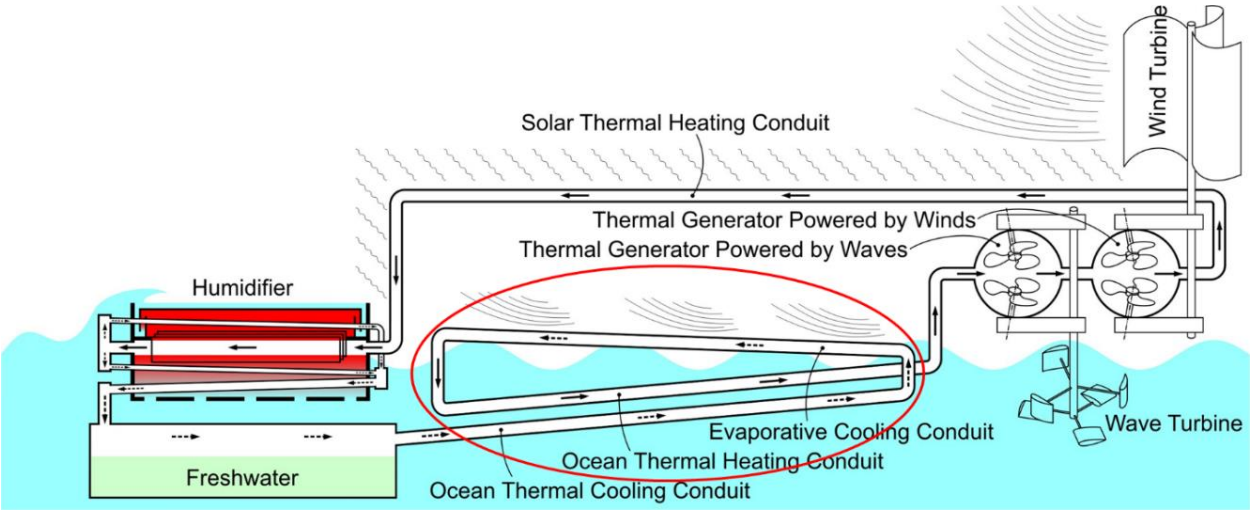

Figure 3: Schematic of a nature-powered ocean-based HDH desalination system [22]. The dehumidification cycle is circled in red. In this system, the dehumidification cycle consists of two stages.

CHAPTER II

OCEAN-BASED DEHUMIDIFICATION FOR HDH DESALINATION

Improvements in the development of HDH desalination systems have been achieved in recent years. Nonetheless, the improvements that have received most attention focus on solar heaters and humidifiers [17, 24-26]. Dehumidification systems have often been adapted from air conditioning condensation systems rather than developed specifically for HDH applications. The main challenge to improve the HDH process lies on improving the overall thermal energy efficiency of the system, and consequently, decreasing the cost of freshwater produced. Previous studies have proposed improvements on the thermodynamic balance [27,28] of the humidification and dehumidification processes that can improve the competitiveness of HDH systems with other technologies. In particular, the dehumidification process holds some of the main challenges on increasing the thermal efficiency and reducing the overall cost of the system. Water vapor diffused on air suffers from large resistance to mass transfer. Additionally, a trade-off between increased heat and mass transfer characteristics and small heat transfer area has to be made.

2.1 Types of dehumidifiers

Dehumidifiers can be divided in two categories: direct-contact and indirect-contact systems. Indirect-contact dehumidifiers rely on cooled solid surfaces in contact with the gas stream. Many studies have been performed using indirect contact dehumidifiers including

conventional condensers such as plate-fin tube heat exchangers, shell-and-tube, shell-and-plate, plate, and finned tube heat exchangers [29-33]. For this type of dehumidifiers one can theoretically achieve high heat and mass transfer by including densely packed solid surfaces with large surface areas. However, due to constraints of cost, weight, and manufacturability the configurations that one can achieve are limited. Additionally, the energy required by the system is directly related to the pressure drop across the dehumidifier, therefore, the geometry and surface area should be optimized to reduce pressure losses. To achieve the most energy efficient dehumidification system, a good mass and heat transfer is necessary without involving a large pressure drop.

Direct-contact heat exchangers rely on the contact between the gas stream and a cooled liquid stream for heat and mass transfer. Direct-contact heat exchangers include spray columns and spray packed-bed condensers. Other novel approaches for direct contact applications that have received increasing attention include bubble columns [34] and string arrays [35]. In recent studies, direct contact heat exchangers have shown promising results on increasing heat transfer on several applications [36-39]. Packed beds have been widely used with gas streams because of the irregular paths help create high heat transfer effectiveness. The main challenges in this technology are the relatively high pressure drops experienced on the gas stream and liquid flooding that constrains gas loadings [38]. Application of spray columns has also been widely studied to achieve high heat transfer rates by dispensing small droplets into the gas stream [37], but they can experience practical challenges: reduced heat transfers due to short residence time of large droplets [40]; and the excessive pumping power required for the spray generation. Bubble columns received recent attention on HDH applications for the potential of achieving high heat and mass transfer. Similar to the spray columns, however, a high-power source is

required to achieve the high pressure necessary to sustain gas flow and overcome the water column leading to increased energy requirements. One technology that has shown promising results is the use of string arrays with liquid running through the strings to create a controlled direct-contact stream of liquid beads without introducing high drag and therefore minimizing pressure drop [35]. Schematics of different types of direct contact dehumidifiers are show in in Figure 4.

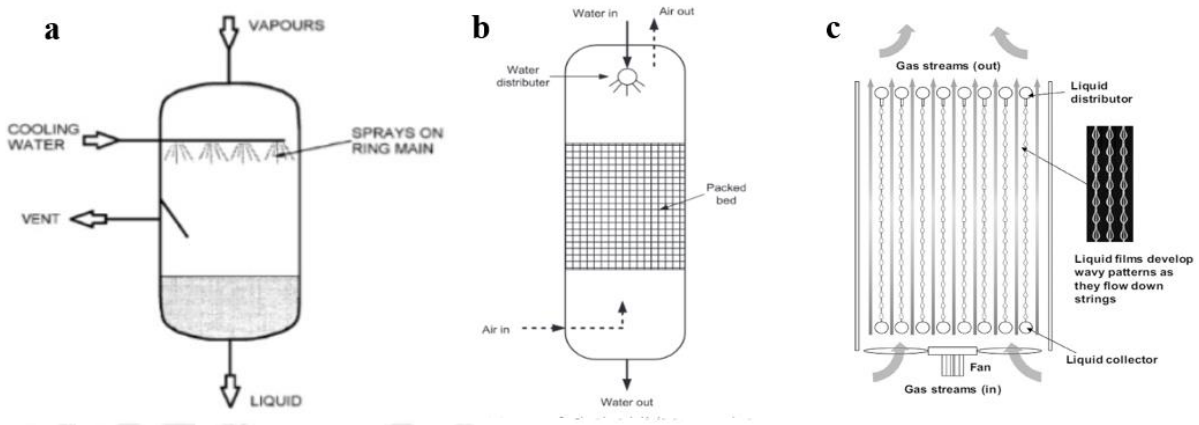

Figure 4: Diagrams of different types of direct-contact dehumidifiers and condensers. a) Spray column, b) packed bed, and c) string arrays.

2.2 Dehumidification using string arrays

String arrays, also called “strings of beads” due to the liquid bead pattern formed on the strings as shown in Figure 4-c, has been widely studied for many applications to enhance heat and mass transfer [35, 41-43]. One of the earliest studies of this approach was done by Hattori et al. in 1994 for thermal energy recovery [43] by feeding liquid onto parallel wires in countercurrent flow to a gas stream. The concept of using string arrays works by introducing liquid to the vertical wires creating beads strung on each wire at regular intervals; if the wire is moderately wettable, a thin film forms to sheathe the wire, thereby interconnecting the beads if

enough liquid flowrate is provided. Since the beads fall slowly due to the shear forces between the liquid and the strings, a sufficient gas-liquid contact time is available improving heat and mass transfer. Early studies have compared the performance of parallel strings direct-contact heat exchangers to spray columns, packed beds, and wetted wall heat exchangers showing improved mass transfer for CO2 absorption applications [42]. More recently, this concept was specifically studied for dehumidification applications by Sadeghpour et al. [35] by supplying cool water to the strings and using hot humid air as the countercurrent gas. In this study, cotton threads are used to provide high shear forces and reduce the velocity of the water running on the vertical wires increasing the liquid-gas contact time. The study provides encouraging results on enhanced heat and mass transfer for the dehumidifier while keeping a relatively low pressure drop compared to other direct and indirect-contact dehumidifiers. The enhanced mass transfer is attributed to the presence of semi-spherical water beads forming on the surface of the strings. The numerical simulation performed in this study results on a mass transfer conductance up to five times higher around the spherical water beads as compared to the substrate, or cylindrical portion of the string that connects the two water droplets. Therefore, a high number of water beads in counterflow of the incoming air, yields a higher effectiveness for the dehumidifier. These findings agree with previous bio-inspired studies that have found improved condensation on localized surface bumps [44]. Dehumidification using parallel strings offers a 200% improvement in the condensation rate per volume than the current states of the art [35]. Enhanced heat and mass transfer at a low-pressure drop is the definite characteristic of a highly efficient dehumidifier, and therefore, the use of wetted strings parallel to the gas flow is a promising configuration for a relatively simple design with enhanced heat transfer characteristics.

All the previous studies using string arrays utilize a reservoir in top of the vertical strings and nozzles to inject the cooling fluid to the parallel vertical strings at a controlled flow rate. The head pressure of the liquid above the strings is injected to induce a controlled flow rate, hence, maintaining a constant flow of water beads along the strings (or wires). By using this method one can control the liquid flow rate in the strings affecting the spacing and size of liquid beads. Studies have shown that the liquid flow rate and gas velocity affect the heat and mass transfer effectiveness, specifically, at low air velocities and increased liquid flow rate on the strings, the heat exchanger effectiveness increases [35,45]. These results are attributed to the increased formation of liquid beads that provide a larger surface area for heat and mass exchange, and the larger contact time between the liquid stream and countercurrent gas flow at low air velocities.

2.3 "Strings-of-beads" for ocean-based dehumidification

The application of parallel string arrays to induce direct contact heat and mass exchange for ocean-based HDH desalination has not yet been studied. For this application, a cold liquid reservoir to induce liquid flow rate on the strings is not practical nor feasible since the cooling liquid is ocean saltwater that cannot be mixed with the freshwater produced. Additionally, the use of small nozzles is not practical due to fouling and calcium deposition that will form and clog such small openings. Therefore, the liquid droplets on the strings are caused by the condensation of the humid air on its cooler surroundings, by indirect contact cooling, and by pinning of the water molecules into the strings. It is well known that for water vapor that is supersaturated in air and shall condensate on a substrate this implies a basic condition: The structure has to be cooler than its environment and has to be maintained as such, or else a hydrophobic or hydrophilic surface can promote condensation of water molecules [46,47,5]. Cooling the walls of a dehumidifier duct is straightforward; indirect contact heat transfer is

caused by the fresh ocean water in direct contact with the walls of the dehumidifier or by combining the wind and ocean water for evaporative cooling. Surface condensation on the other hand, requires much more careful consideration of material surface wettability in order to promote the most efficient water droplet formation and movement.

2.3.1 Surface wetting

It is well known that the surface wettability properties play a major role in the formation and mobility of water droplets in the presence of water vapor, and consequently can affect heat transfer equipment [48]. Surface wettability refers to the hydrophilic or hydrophobic characteristics of the surface. Hydrophilic surfaces refer to surfaces that create a low contact angle with water (< 30°) and hydrophobic refers to large contact angles (>120°) as seen in Figure (5). Superhydrophobicity often refers to surfaces that are able to create a contact angle over 150° up to a full droplet separation from the surface.

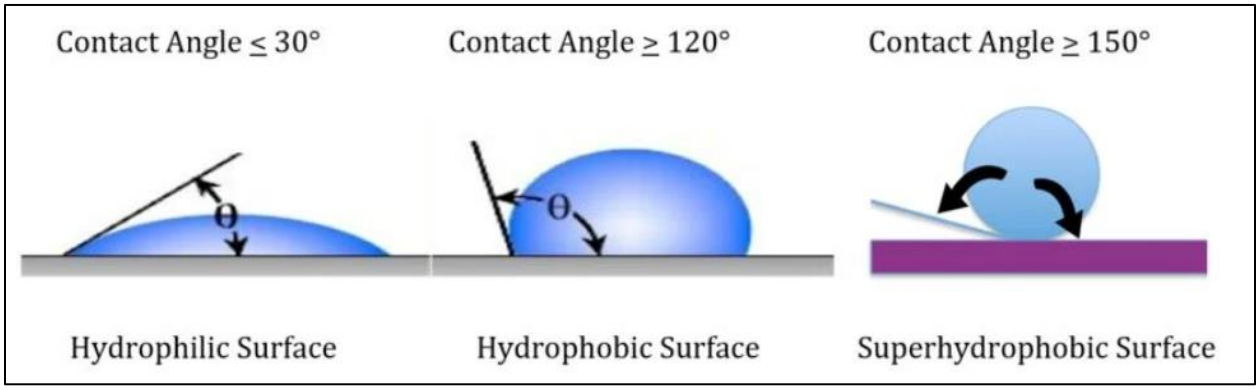

Figure 5: Contact angle of water droplet in hydrophilic, hydrophobic, and superhydrophobic surfaces.

In heat transfer engineering, the wettability of contact surfaces for heat exchangers has been widely studied. Filmwise condensation (FWC) on heat transfer surfaces create a condensate layer that acts as an insulating barrier between the two fluids as seen in Figure (6). For indirect

contact heat exchangers, superhydrophobic surfaces with high droplet mobility are preferred for increased efficiency in heat transfer [49-52].

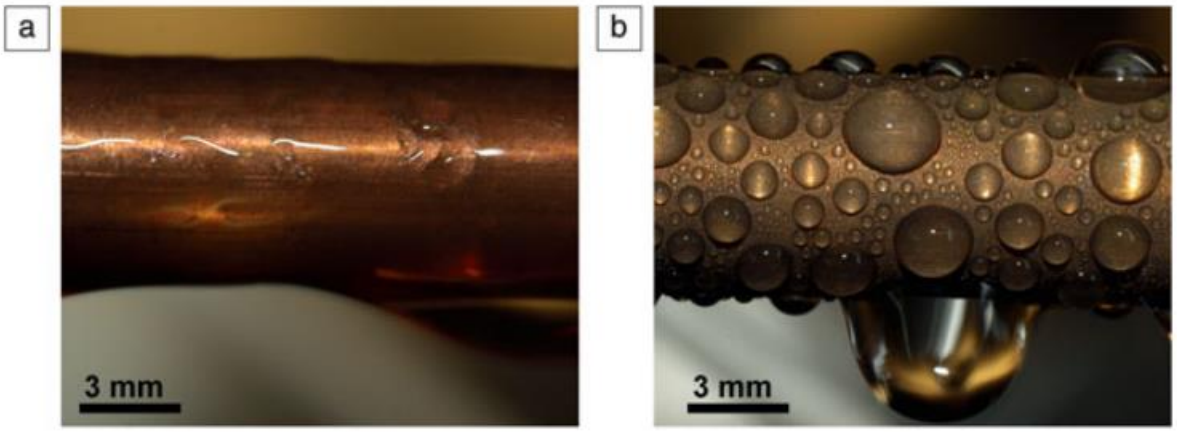

Figure 6: Images of (a) filmwise condensation on a smooth hydrophilic Copper tube, and (b) dropwise condensation on a coated copper tube.

The natural wettability of a surface can be altered through chemical manipulation of a surface, or by selectively altering portions of a surface texture [53]. Super-hydrophobicity has been previously studied based on the lotus effect [54] which utilizes micro/nanostructures to create air pockets between the solid-water contact. The trapped air creates a high surface energy that allows the water droplets to roll away easily. The enhanced mobility of water droplets has demonstrated to improve the heat transfer on dropwise condensing (DWC) applications. On the other hand, bioinspired water collection technologies have found living examples that promote condensation on hydrophilic surfaces. For example, the hydrophilic skin of several lizards that promote water absorption from the humid air and the condensed water can easily move due to a capillary network on their skin [55], and the hydrophilic nature of spider silk that allows the formation and collection of water droplets due to the spindle-shaped knots on the silk strings

[56]. Bio-inspired studies have replicated similar structures to combine the improved nucleation of hydrophilic surfaces with high water droplet mobility to improve humidity collection. Results have shown a higher nucleation rate on hydrophilic than hydrophobic surfaces.

Existing methods that combine hydrophilic surfaces with high droplet mobility have use three driving forces. 1) Simultaneous high nucleation and droplet mobility inspired on the spider silk is achieved due to the Laplace pressure gradient [56]. 2) Surfaces with high wettability gradient can promote the movement of water droplets without external forces from the hydrophobic to the hydrophilic region [57,58]. 3) Utilizing a combined hydrophobic-hydrophilic surface taking advantage of mixed wettability patterns [59]. Various studies have demonstrated high nucleation density and improved condensate droplet movement on fabricated surfaces with mixed wettability patterns [60,61]. Findings agree that the optimal conditions to enhance heat transfer when vapor condensation is present is a high nucleation ability and efficient droplet mobility. All previous studies mentioned above have studied the fabrication of custom made micro or nano structures to enhance the wettability properties of the studied materials. Additionally, in some cases to achieve such improved wettability properties a lubricant is necessary over the solid surface to improve water droplet mobility [44]. The application of such micro/nano-modified surfaces is often impractical for heat transfer equipment since they can lose their effectiveness over time due to abrasion, corrosion, or fouling which are common conditions inside heat exchangers. The use of lubricants or chemicals to alter the surface wettability is also impractical in applications for freshwater production due to the contamination of the produced freshwater. Most commercially available materials of practical interest are neither completely wetting nor non-wetting. The effectiveness of using a bundle of parallel strings inside a

dehumidifier is therefore directly linked to the surface properties of the strings and how these promote high nucleation rates and high droplet movement along the strings.

In summary, for surface induced condensation, the use of hydrophobic surfaces is advantageous due to the large water contact angles that ensure DWC and efficient droplet departure ability. On the other hand, hydrophilic surfaces present more efficient nucleation and can effectively trap water molecules in low-humidity conditions. In general, it has been observed that DWC forms on hydrophobic surfaces and FWC forms on hydrophilic surfaces. For this study the possibility of creating the strigs-of-beads effect by pining of the water molecules and sliding of the water beads on various string materials is studied. Hence, the ocean-based dehumidifier is designed to present indirect and direct contact dehumidification simultaneously; the first by the fresh ocean water surrounding the duct (i.e. either submerged or by evaporative cooling), and the former by the sliding water beads on the strings in contact with the incoming humid air. This configuration can potentially increase heat and mass transfer resulting on increased freshwater produced as opposed to using only indirect-contact dehumidification. Additionally, the use of parallel strings longitudinally to the air flow, provides clear paths for the air minimizing pressure drop as has been shown by Sadeghpour et al [35].

2.3.2 Axial gas flow along cylindrical surfaces

Axial gas flow along the strings can be compared to the highly studied case of axial flow across parallel cylinders [62,63] as shown in Figure 7. The use of cylindrical surfaces parallel to a flow has many heat exchanger applications. Studies on longitudinal cylinder flow mainly focus on the configuration of the cylinders and their relation on heat transfer and pressure drop. Studies show that a triangular shaped array increases heat transfer compared to a square configuration.

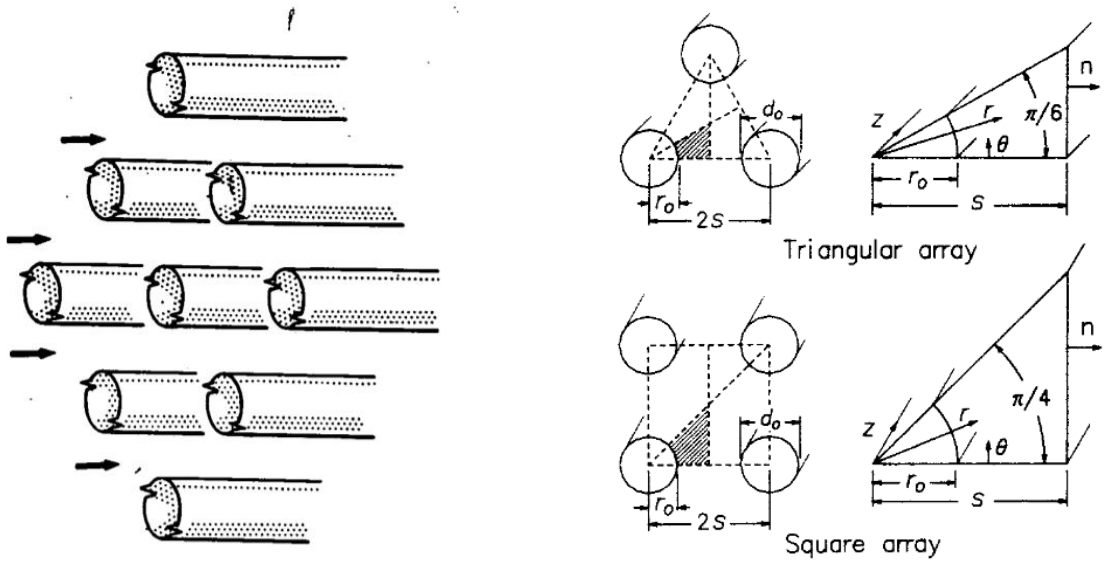

Figure 7: Diagrams showing the two different configurations in the study of axial flow through a bundle of parallel cylinders. Square array and triangular array configurations.

However, at large pitch-to-diameter ratios of $s/r_o > 4$ (here, s is one half the distance from the centerline of two adjacent cylinders and r_o is the radius of the cylinder), the configuration of the cylinders has a negligible effect on the heat transfer coefficient. For this study, the small diameter of the strings (this study focuses on strings with a dimeter of less than 1mm) present very high pitch-to-diameter ratios (s/ro > 8), therefore the geometric configuration of the strings has a negligible effect on the heat transfer coefficient. An increase on heat transfer characteristics is noticeable after a pitch-to-diameter ratio of 2 and below, which only applies to larger diameter and highly packed heat exchangers. Similarly, the geometry of the cylinders has a negligible effect on shear forces at pitch-to-diameter ratios above 4 concluding that the arrangement of the strings has little effect on the pressure drop characteristics of the dehumidifier. For his study, a square arrangement was used.

2.4 Dehumidifier analysis

The dehumidification process holds some of the main challenges on increasing the thermal efficiency of the HDH system. Water vapor diffused on air suffers from large resistance to mass transfer. To achieve the most energy efficient dehumidification system, a good mass and heat transfer is necessary without involving a large pressure drop on the air. Decreasing the pressure drop across the system benefits the overall energy consumption. To understand the parameters that affect the pressure drop and heat/mass transfer across the system it is imperative to not only consider solid surface contact areas but also the hydraulic characteristics of the system are important since the air-liquid interface can greatly affect the heat and mass transfer characteristics and pressure drop. For the following sections, symbols will be used to refer to the properties of moist air which is the fluid of interest in the present study. A summary of the utilized symbols is shown in table 1. Symbols with the subscripts *a* and *v* denote corresponding properties of air and water vapor, respectively. The subscript *w* is used to refer to the condensate fresh water produced in the dehumidification process. Symbols with no subscripts represent the properties of moist air as a mixture.

Table 1: Symbols used for dehumidifier analysis.

Nomenclature	**Subscripts**
T temperature, K	*a* air
$\dot{m}$ mass flow rate, Kg s^{-1}	*v* water vapor
H enthalpy, J kg^{-1}	*w* water produced
D_h hydraulic diameter, m	*sw* seawater
Q energy (heat flow), W	
h_t heat transfer coefficient, W m^{-2} k^{-1}	**Greek symbols**
A area	Φ relative humidity
P pressure, Pa	ω humidity ratio, kg kg^{-1}
V velocity, m s^{-1}	ρ density, kg m^{-3}
	μ viscosity, Pa·s

2.4.1 Thermofluids analysis of dehumidifier

To support the experimental data obtained in this study, some basic analyses have been performed to compare to the experimental results. The main parameters of interests are pressure drop and water production. The HDH process employs dry air as a medium to absorb water vapor and form moist air. The amount of water vapor that air may contain at a specified temperature and pressure reaches the maximum at saturation, and the corresponding relative humidity (RH) is 100%. The water absorption capability of air increases at increased temperature. Temperature and RH of air are important because the thermophysical properties of air such as the density, viscosity, thermal conductivity, specific heat, and thermal diffusivity vary significantly at different temperatures and values of RH [64]. It is important to account for the changes in the thermophysical properties of air in the calculations to minimize the error. Expected temperature and pressure ranges for a typical HDH system are between 10 °C – 80 °C at constant ambient pressure. At this range of temperature and pressure the moist air, dry air, and water vapor follow the ideal gas law with enough accuracy and the thermophysical properties of air can be obtained using linear superposition at the corresponding parameters [65]. As the humid air passes through the dehumidifier, temperature will decrease to produce the freshwater.

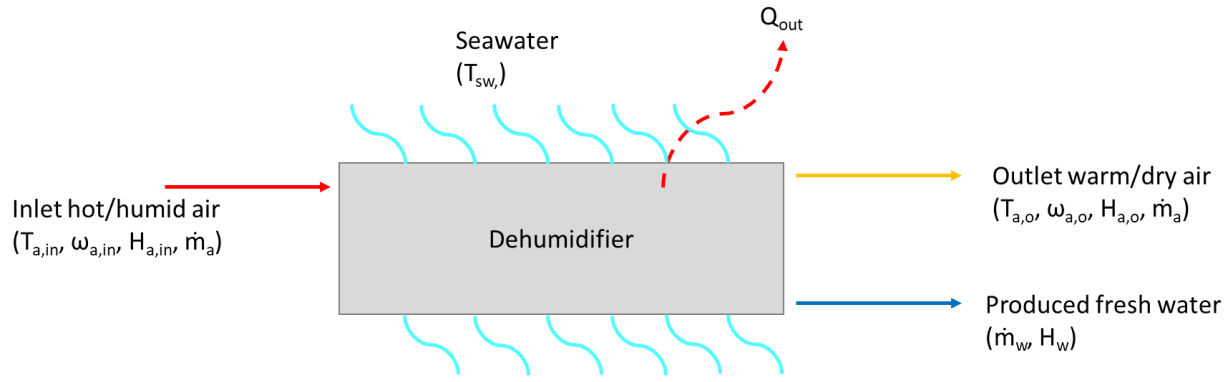

Figure 8: Heat and mass balance parameters for an ocean-based dehumidifier.

During this process the mass flow of dry air remains unchanged, whereas the amount of humid air and the amount of condensate change. In the dehumidifier, the hot humid air and the seawater are not in direct contact. The humid air moves through the space between the strings and the walls of the dehumidifier. During the dehumidification process, the sensible and latent heat is transferred from the hot humid air stream to the seawater. A schematic of the control volume diagram and parameters of the dehumidifier is shown in Figure 8.

The humid air enters the dehumidifier at operating conditions of temperature ($T_{a,in}$), humidity ratio ($\omega_{a,in}$), enthalpy of humid air ($H_{a,in}$) and the mass flow rate ($\dot{m}_a$). While the air exits the dehumidifier at temperature ($T_{a,o}$), humidity ratio ($\omega_{a,o}$), and enthalpy of humid air ($H_{a,o}$). The seawater is introduced at a constant temperature (T_{sw}).

The energy balance in the dehumidifier can be written as follows:

$$Q_{out} = \dot{m}_a\left(H_{a,o} - H_{a,in}\right) - \dot{m}_w H_w \quad (1)$$

With known inlet and outlet temperature and relative humidity, the humidity ratio can be obtained by means of linear superposition of the corresponding air and water vapor psychrometric properties to obtain the overall water produced by the condensation of water vapor:

$$\dot{m}_w = -\dot{m}_a(\omega_{a,in} - \omega_{a,o}) \quad (2)$$

To simplify the unit conversion and maintain constant units throughout the calculations, equation (2) can be represented as follows [18]:

$$\dot{m}_w = \frac{3600\,(\omega_{a,in} - \omega_{a,o})\dot{m}_a}{.998(1+\omega_{a,o})} \quad (3)$$

Where $\dot{m}_a$ is in kg/s and $\dot{m}_w$ is in l/h of liquid water. Condensation occurs at 100% RH, hence, the humidity ratio decreases with decreasing temperature which causes the fresh water production.

2.4.2 Pressure drop

The calculations for the pressure loss in the dehumidifier require de determination of the air and water vapor properties; the density ρ (kg/m^3) and viscosity μ (in Pa·s) of the air at a specific temperature (K), pressure (Pa), and humidity ratio can be determined using the following equations [18]:

$$\mu = \frac{\mu_a}{1+0.3519\left[1+0.8881\left(\frac{\mu_a}{\mu_v}\right)^{0.5}\right]^2 \cdot \omega} + \frac{\mu_v}{1+0.1727\left[1+1.1260\left(\frac{\mu_v}{\mu_a}\right)^{0.5}\right]^2 / \omega} \quad (4)$$

$$\mu_a \cdot 10^6 = 0.40401 + 0.074582T - 5.7171 \cdot 10^{-5}T^2 + 2.9928 \cdot 10^{-8}T^3 - 6.2524 \cdot 10^{-12}T^4 \quad (5)$$

$$\mu_v \cdot 10^6 = \frac{\sqrt{\frac{T}{647.27}}}{0.0181483+0.0177624\left(\frac{647.27}{T}\right)+0.01015287\left(\frac{647.27}{T}\right)^2} - 0.0036744\left(\frac{647.27}{T}\right)^3 \quad (6)$$

$$\rho = \frac{1+\omega}{461.56(0.62198+\omega)} \cdot \frac{p}{T} \quad (7)$$

After determining the ρ and μ, the pressure loss can be calculated using equation (8). For simplified calculations the flow is assumed to be fully developed, and the pressure drop due to condensation in neglected:

$$Re = \frac{\rho V D_h}{\mu} \quad (8)$$

The Darcy friction factor for turbulent flow can be determined:

$$\frac{1}{f^{1/2}} = -2.0\, log\left(\frac{2.51}{Re\, f^{1/2}}\right) \quad (9)$$

$$\Delta P = \frac{fL\rho V^2}{2D} \quad (10)$$

In these equations Re is the Reynold's number, V is the average flow velocity of the air, D_h is the hydraulic diameter, L is the dehumidifier length, ε is the wall roughness and f is the Darcy friction factor. For an approximate calculation of pressure loss along the length of the dehumidifier, since there are variations of temperature, humidity ratio, density, viscosity and other parameters, the air properties are calculated at the known inlet and outlet conditions and the average value is used for the calculations. This procedure for the calculations may add additional error to the pressure drop calculations, however, the purpose of the calculations is only to verify the values provided by the instrumentation. Additionally, the values will be compared to other comparable systems to additionally support the results from this investigation.

2.4.3 Effectiveness

In a heat and mass exchanger, different equations have been developed to measure effectiveness. For dehumidification systems the most general equation to measure effectiveness is the ratio of actual heat transfer amount to maximum heat transfer amount [66-68]:

$$\eta = \frac{Q_{act}}{Q_{max}} \quad (11)$$

Since the heat transfer properties of the material and the surface area can be assumed to be the same in the top and bottom of the ratio, the equation can be simplified to the ratio of the actual temperature difference, divided by the maximum theoretical temperature difference that can be achieved (i.e. the air exists at a temperature which is the same as the ambient outside temperature):

$$\varepsilon = \frac{T_{a,in} - T_{a,o}}{T_{a,in} - T_{ambient}} \; x \; 100\% \quad (12)$$

Equation (12) will be utilized to measure the effectiveness of the system at varying flowrates across the dehumidifier.

2.5 Objective of the present study

This study will set the foundation to demonstrate the effect of a bundle of parallel strings inside an ocean-based dehumidifier for HDH desalination applications. The study will use a bundle of parallel strings of various materials inside an inclined dehumidifier duct to induce DWC or FWC and form droplets that simulate the strings-of-beads effect. The presents study aims to (i) study and understand the parameters that characterize a cooling dehumidification system for ocean-based HDH applications, (ii) experimentally test the simultaneous heat and mass transfer of a direct and indirect-contact dehumidifier that utilizes thin strings of various commercially available materials with the presence of a counterflowing gas stream and (iii) to compare the dehumidifier effectiveness and gas-phase pressure drop with the different string materials.

CHAPTER III

TESTING PROTOTYPE DESIGN AND EXPERIMENTAL PROCEDURES

The design parameters, equipment, and testing plan of the necessary apparatus to analyze the dehumidification process are discussed in the following paragraphs.

3.1 Design requirements

As mentioned in the previous chapters, a highly energy efficient dehumidification system is characterized by a high rate of heat and mas transfer while maintaining a low pressure drop. Based on large amounts of research done on HDH systems in the last years, the most energy-efficient is the closed-air open-water cycle [17]. Additionally, increased thermodynamic efficiency has been proven to be achieved for dehumidification by using wetted strings parallel to the flow for increased mass and heat transfer without a large pressure drop. Therefore, based on the findings of previous research, this study will focus on building and testing a dehumidifier for closed-air open-water applications with a bundle of parallel strings in various materials. To make the design suitable for ocean-based applications, the design targets a simple and robust design that requires no electric or electronic components for cost-effective and practical applications. The main source of thermal energy comes from sea water for cooling and dehumidification. The testing prototype will be tested in a controlled laboratory environment to determine the effect of parallel strings on the water production of the dehumidifier.

3.2 Material selection

Materials for the testing prototype were selected based on durability and reliability at moderately high temperatures (e.g. 60 C). The material for the dehumidifier duct was chosen based on good heat transfer characteristics, high corrosion resistance and availability. Fouling resistance is also a factor that needs to be considered in the material selection, especially for ocean-based applications due to the high mineral concentration of the seawater.

3.2.1 Fouling

Fouling is a long-term effect that must be considered when selecting materials that can keep long term efficiency. In the case of ocean-based HDH systems, fouling occurs both inside and outside of the ducts. Inside of the ducts is caused because water-soluble salts like calcium get mixed during the humidification process on the humid air and are dispositioned over time inside of the ducts of the dehumidification. On the outer walls fouling is caused by the constant contact of seawater and the dehumidifier walls. The deposition of salts and calcium is a common problem on desalination systems and the fouling accumulation decreases the system's efficiency, increases pressure drop, and increases maintenance costs [69,70]. Additionally, for ocean-based applications that require long term reliability with limited access for maintenance it is important to avoid narrow and/or small openings such as nozzles and diffusers due to the rapid accumulation of solid deposits and clogging of such openings.

Studies have shown that fouling increases on materials with higher surface free energy. Additionally, on materials with higher thermal conductivity also increase fouling deposition. In a comparison between 316 SS, brass and aluminum, the stainless-steel sample showed the lowest fouling disposition and Aluminum showed the highest fouling deposition [70]. However, the

thermal conductivity of metals is not highly compromised when fouling occurs, only decreasing by less than 10%. For this reason, high conductivity materials may be preferred for the construction of ocean-based dehumidification ducts. Mineral deposition inside the dehumidifier can be considered negligible since it has been shown that there is less than 9% decrease on the overall heat transfer coefficient of the material after reaching maximum fouling. For the outer fouling, although the resistance changes over time, constant values are recommended for the design in the literature [71].

3.2.2 String tension testing

Different materials of strings were tested to determine their long-term performance. The material differences are shown to have different properties that affect their ability to absorb and retain water, hold water droplets, and withstand temperature changes without losing tension. Tension retention is a particularly important characteristic for the strings since the strings should remain parallel to each other inside of the dehumidifier duct for long periods of time. The strings losing tension would deform the strings (i.e. like a simply supported beam with a u-deflection) making the parallel string arrangement ineffective and introducing obstructions for the flow of air. Tension retention was experimentally tested using 14 commercially available strings of different materials and diameters to select an appropriate string material for dehumidifier testing. Table 2 summarizes the strings that were used for this test. Two of the tested strings; monofilament nylon fishing line, and zinc-galvanized steel wire, are excluded from this section's data since these materials are already known to retain their tension exceptionally well. The tension-retention testing was primarily performed with commonly used sewing string materials with hydrophilic porous surfaces to compare to the monofilament nylon and steel wire during dehumidifier testing.

Table 2: Strings used for tension retention testing. Strings were selected among a variety of commercially available materials of strings used for crafts, sewing, and embroidery.

Description	Material	Diameter (mm)
Brown	100% Hemp	0.8
Green #1	100% Nylon	0.37
White #1	100% Polyester	0.36
Golden #1	61% Polyester 39% Cotton	0.4
Cheese rope	100% cotton thick rope	1.75
Green #2	100% cotton twisted	1.11
Golden #2	100% cotton 6x#25 strand	0.92
White #2	100% Polyester sewing thread	0.44
No 8 Cotton	100% Cotton	0.7
No 5 Cotton	100% Cotton	0.95
White #3	75% Polyester 25% Cotton	0.55
Yellow	100% Polyester	0.6

The test was performed by tying 1.8-meter-long strings to each end and measuring how much tension the strings retain after 120 hours under outdoor environmental conditions. Figure 9 shows a picture of the experimental setup. Additionally, to mimic the conditions of the strings inside of the dehumidifier, the strings were sprayed until fully wetted with water to form water beads around the strings; wetting cycles were repeated every 12 hours. The test was performed outdoors during similar weather days to allow temperature changes to affect the strings to test their durability and tension retention when exposed to humidity and temperature changes.

The distance from the center of the strings to the fixed point was measured every 12 hours with a caliper and recorded to identify the strings that hold tension better after several days. Each measurement was repeated three times and the average measurement was used.

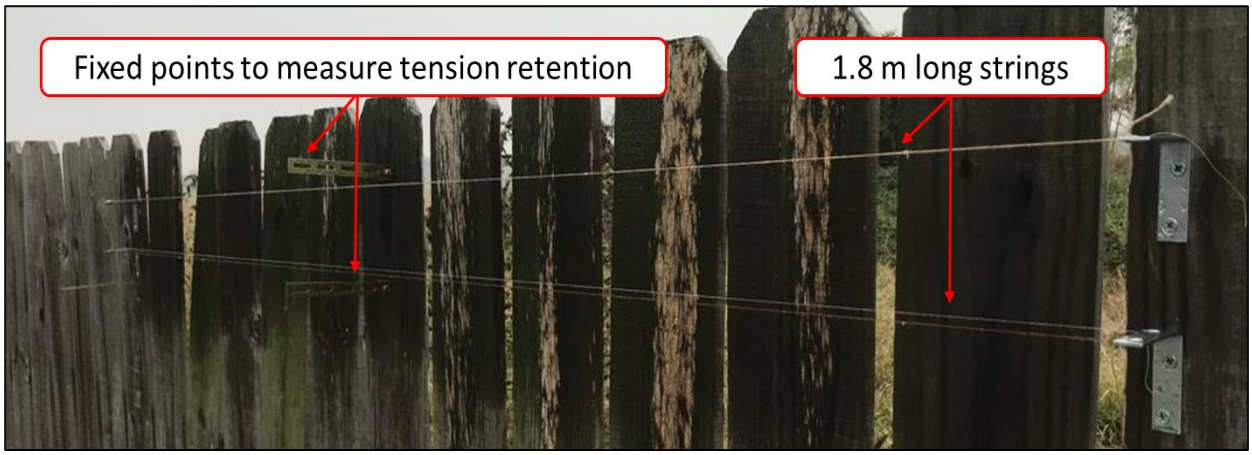

Figure 9: Experimental setup to test tension retention of 12 strings of various material compositions.

Furthermore, the spraying also allowed the formation of water beads on the strings and the bead formation was compared between string materials. The data was plotted to visually represent the elongation at the center of the strings as a function of time as seen in Figure 10.

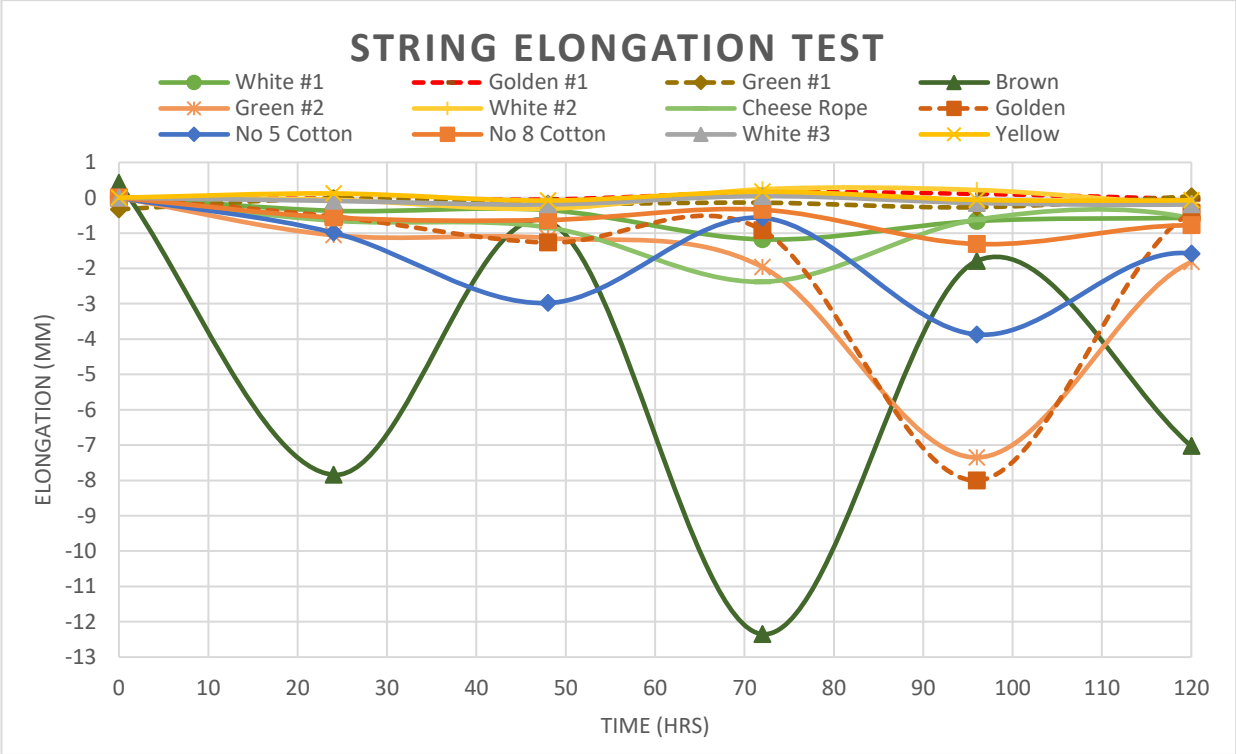

Figure 10: Elongation at the center of 1.8m long strings during a 120-hour period.

The data clearly shows which strings retain their tension better over several days. The overall behavior of most strings is to expand and contract as seen in Figure 10. 100% cotton strings did not perform as good as the ones containing polyester or nylon. 100% polyester and cotton-polyester mix strings performed the best retaining tension over several hours without much variations. The best performing strings were selected as the ones with an elongation less than 0.5 mm, these 5 strings are compared in Figure 11.

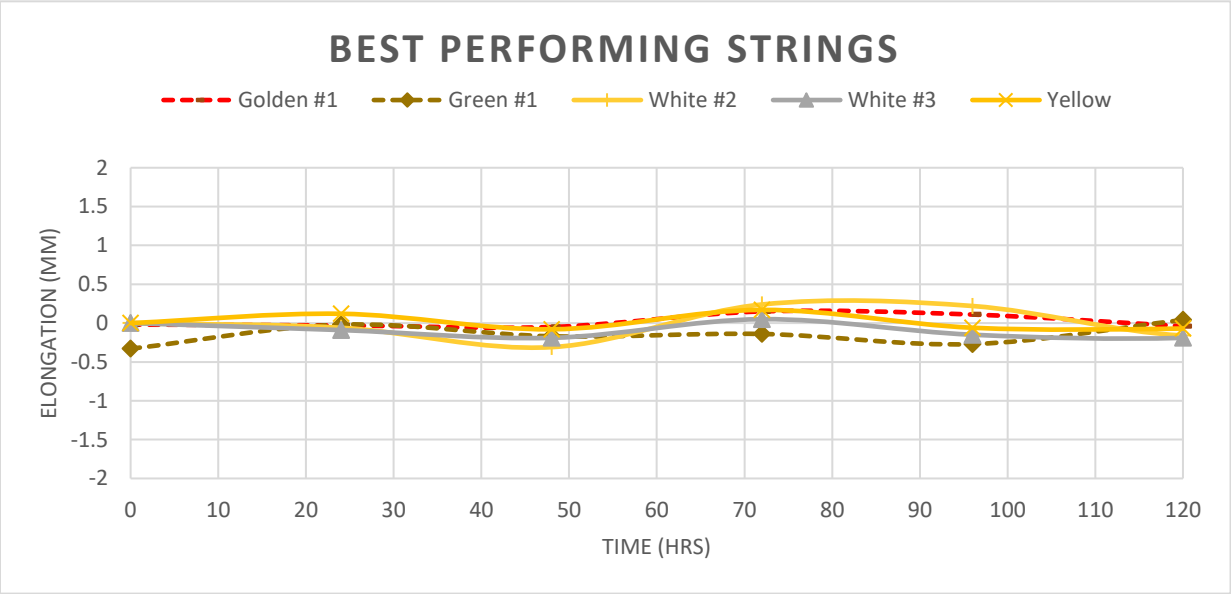

Figure 11: Best performing strings that showed a variation of less than 0.5mm of deflection at the center of the string during a 120-hour period.

The materials of the best performing strings during the tension retention testing are showed in table 1. As seen on Figure 11, none of the best performing strings are 100% cotton material. The strings that showed best tension retention all are 100% polyester or polyester-cotton mix, and one 100% nylon (similar to monofilament nylon fishing line, nylon twisted strings have high elasticity, improving the tension retention). 100% cotton and hemp materials showed to lose their tension over time no matter their diameter and twisting geometry, hence, their lack of tension retention can be attributed to the material. For this reason, polyester

containing strings are preferred for the experimentation. Additionally, to increase durability and reliability of the strings over time, only strings with a diameter of over 0.5 mm were selected, thus ensuring the braking resistance of the strings. With this criterion in mind, the selected string for testing was White #3, a commercially available poly-cotton string that showed excellent tension retention over time. Another important factor to consider is the water bead formation on the surface of the strings. All strings were tested by spraying water every 12 hours and taking pictures to compare water bead formation on the strings. All string materials, without exception, showed the formation of water beads along their surface. In general, the larger the string diameter, it can hold larger water droplets. However, the main variation is in the number of strings that each material forms when fully saturated with water.

Figure 12: Two of the best tension retention strings showing the water bead formation after fully wetting. Poly-cotton mix (White #3) in the top and 100% Polyester (Yellow) on the bottom.

Figure 12 shows an example of the bead formation on two strings of similar diameter but different material composition. As shown in Figure 12, the Yellow (100% Polyester) string, shows an increased formation of water beads around the string and similar water bead size. The difference in number of beads may be attributed to the absorbent nature of cotton material

absorbing more water within its fibers and forming less water beads on the outside. Testing shows that less absorbent material presents higher number of water beads on the surface of the string. The Poly-cotton string was selected for further testing to compare to less absorbent string materials performance. 100% monofilament nylon fishing line with a diameter of 0.47 mm and zinc-galvanized wire with a diameter of 0.58 mm were also used for testing to contrast the results between varying string materials, surface roughness, absorption, and thermal conductivity.

3.3 Experimental setup

In this work, a dehumidifier with the capability of adding a bundle of parallel strings was built to experimentally investigate its performance. The experimental setup was first designed as a 3-D model to ensure fit of the parts and components. Each part was carefully machined with low tolerance to ensure tight fit to prevent leakage. Figure 13 shows the three-dimensional render of the humidification and dehumidification setup as it was designed using siemens NX software. Since the application of this thesis is mainly focused on ocean-based cooling and dehumidification, the testing prototype requires to be inside of a large water tank to be able to wet the outside surface of the duct to simulate ambient freshwater conditions on the outer walls of the dehumidifier. Therefore, the dehumidifier duct was built taking into consideration the dimension constraints of the water tank in the lab and availability of materials in the market. Materials for the testing prototype were selected based on durability and reliability at moderately high temperatures since humidification can range between 40°C – 85°C. 6061 Aluminum was chosen for the material for the dehumidifier due to its good heat transfer characteristics, high corrosion resistance, and availability. Polycarbonate was used for other specific components that needed machining since it has a working temperature range of -40°C – 115°C. Mineral wool thermal insulation with a 3in thickness was used to decrease heat losses on the connecting duct

between the humidifier and dehumidifier. The arrangement of the experimental setup is shown in Figure 13. The flow path of the air includes a (I) humidification to achieve a specific humidity and temperature of air and (II) dehumidifier which collects the condensed freshwater produced. The dehumidifier setup was designed with the ability of inclining the duct from 0-40 degrees to test at various inclination angles.

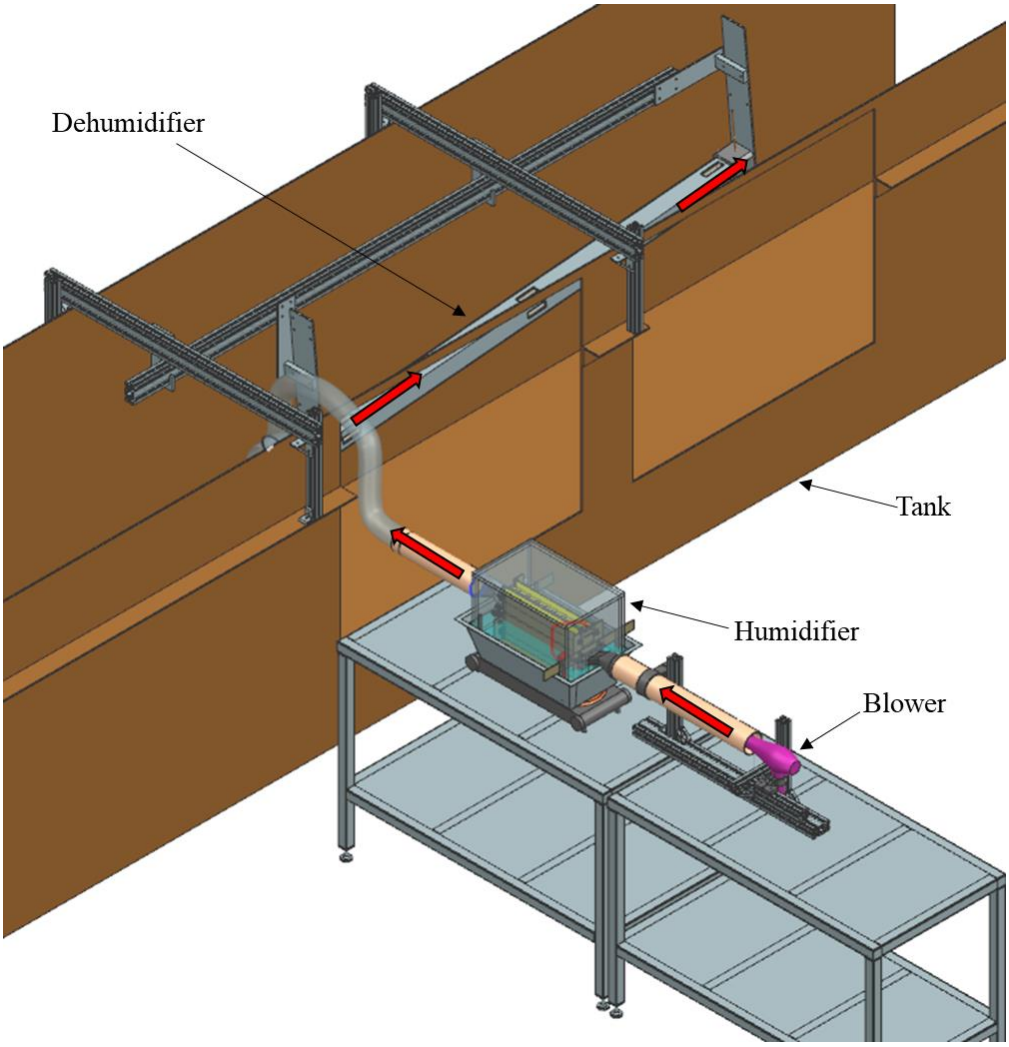

Figure 13: Three-dimensional rendering of the humidification dehumidification experimental unit designed for this study. The arrows show the airflow path at the inlet and outlet of the humidifier and dehumidifier.

We use a humidifier that utilizes wet cotton fabric layers parallel to the airflow as shown in Figure 14. The cotton fabric is continuously wetted with heated water maintained at 56-60 °C by using an overtopping pump to ensure uniform temperature distribution on the fabric. Water temperature in dehumidifier is maintained using a 900-Watt electric stove with two variable temperature burners. The cross-sectional area of flow through the humidifier is 18mm x 48.5mm with 8 layers of fabric evenly spaced in the cross-sectional area of the path of flow. A variable flow hot air blower is used to supply air at 90°C into the humidifier at different air velocities. The humidifier was designed to be 100% efficient (approximately 100% RH) for low flow velocities ranging from 0.1 – 1.5 m/s. A bundle of parallel straws with inner diameter of 5 mm is used upstream of the humidifier to create a uniform flow. A humidity sensor is used downstream of the humidifier to monitor humidity of air. The humidified air then flows through an aluminum insulated duct with a diameter of 76mm that connects to the dehumidifier.

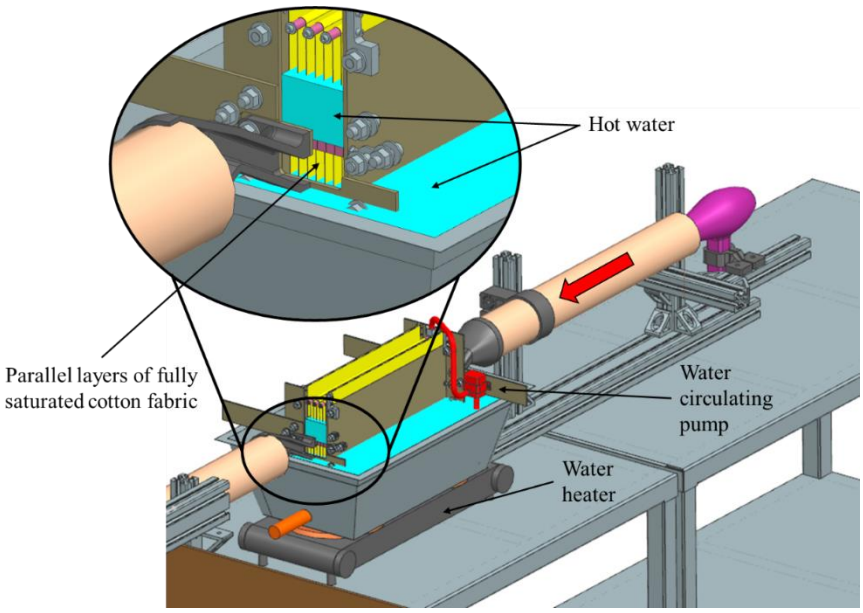

Figure 14: Three-dimensional rendering of the humidifier used for this study. Eight parallel layers of cotton fabric are maintained fully saturated with hot water to ensure efficient mixing of air passing through the channels. The arrow shows the airflow direction at the inlet.

The dehumidifier consists of a 1.8 m-long inclined square aluminum duct with a 71 mm-side. The duct was designed to add up to 121 strings in a square array with a 5.8mm pitch. The inclination of the duct allows the produced freshwater to flow back to a freshwater collecting reservoir located at the inlet of the dehumidifier duct as seen in Figure 15. An aluminum beam structure was designed to hold the dehumidifier duct at varying angles inside the water tank. Strings were selected based on the criteria specified in section 3.2.2. The dehumidifier is placed in a water tank measuring 1.3m tall by 1m width and 15m long to maintain working area dry during testing.

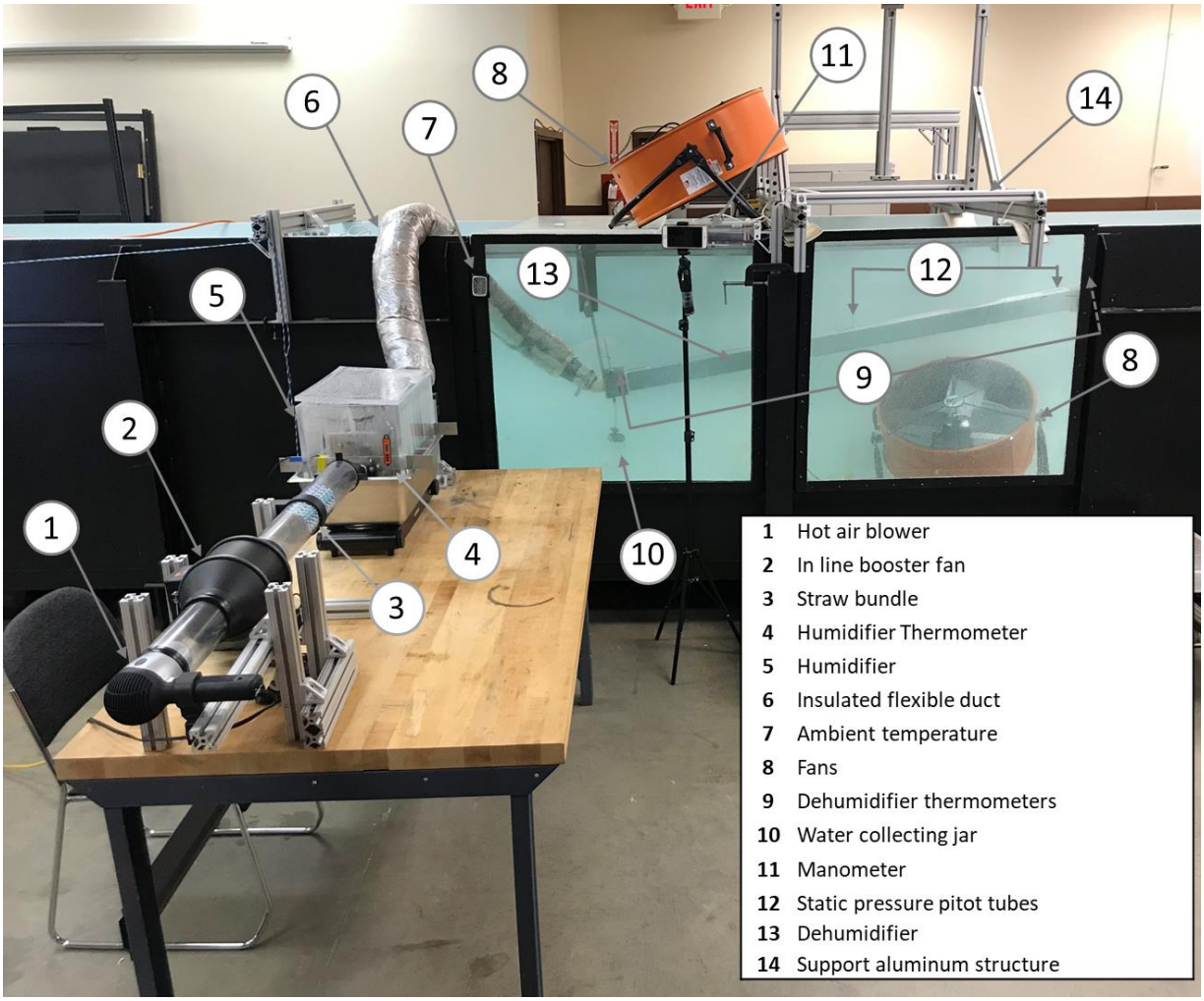

Figure 15: Experimental setup used for the testing in this study.

Evaporative cooling was used for all experimental runs to maintain the outer surface of the dehumidifier duct at ambient temperature. Evaporative cooling is created by using two 24in electric fans for ambient air flow movement and manually controlling ambient temperature water at 20 ± 2 °C, spraying to wet the outer surface of the duct periodically. 1500ml of water are sprayed during each 10-minute test. Three sets of liquid glass thermometers are used to monitor the water temperature on the humidifier and the air temperature on the dehumidifier. One measures the humidifier water (submerged by 5 cm), and two are mounted in the axial locations of 0.05 and 1.8 m from the entrance of the dehumidifier to monitor inlet and exit air temperatures. A differential pressure manometer is used to measure air stream pressure drop and flow velocity. For flow velocity a total pressure and static pressure pitot tube combo are located 10 centimeters from the outlet of the duct to measure the maximum velocity. To measure pressure drop, two static pressure pitot tubes are located along the last 0.85-meter-long section of the dehumidifier duct to allow for the air flow to develop and collect accurate static pressure readings as seen in Figure 15.

3.4 Data acquisition

For each test run, water temperature in the humidifier is first adjusted at 58 ± 2 °C and the blower is turned on to induce hot air flow rate through the humidifier. A waiting time of 30 minutes is used before each test to ensure even temperatures throughout the system before each test. Liquid in glass thermometers with a temperature range of -10 – 110 °C are used for temperature measurements with an accuracy of ±1 scale. Laboratory ambient temperature is maintained between 68 – 72 °C to ensure uniformity of testing. Pressure drop and maximum velocity are measured by using 2mm outer diameter pitot tubes connected to an inclined liquid manometer. A liquid manometer gauge with a range of 0 – 0.25 WC with an accuracy of ±2%

was used. After reaching steady state, testing time was 10 minutes. Water produced after each test was measured using an electronic scale with a 0.01g accuracy. Each test was repeated three times to ensure repeatability of results within 5%.

CHAPTER IV

RESULTS AND DISCUSSION

All previous studies that have implemented strings for enhanced heat and mass transfer have utilized a controlled flowrate of liquid down the strings counterflowing the incoming gas [35, 41-43]. The flowrate of liquid down the strings along with the shear forces between the liquid and the string surface provide the ability of controlling the formation of water beads downs the strings resulting in a controlled contact time between the liquid and the gas, hence, improving the heat and mass transfer between the two. Unlike all previous testing that use a bundle of parallel strings, this study targets to study the effect that the strings-of-beads have on the heat transfer and water production of a dehumidifier when the string-wetting is caused only by the humidity of the air passing through the strings. Another important difference is the inclination of the strings, all previous studies have used vertical strings. For practical reasons and for ideal ocean-based applications, the preferred position of the dehumidifier is nearly horizontal or inclined to avoid the system to submerge too deep in the water.

For this study, the materials of the strings for testing were selected to contrast the effect that different surfaces have on water bead formation and sliding on inclined strings and how that can affect humid air condensation. The results of the experimentation and calculations are compared and discusses in this section.

4.1 Flowrate measurements

Water production is directly proportional to the amount of humid air that flows through the humidifier duct. Constant air flowrate during testing is necessary to make each testing comparable and reliable. The use of flowrate meters is not an option because of the flow distortion and pressure drop that the instrumentation requires to accurately measure flow. To minimize flow interference small diameter pitot tubes were used to measure the maximum velocity at the center of the duct. Before and after each test velocity measurements were performed during a 15-minute timeframe to ensure the stability of flow along the center streamline. Two flowrates are mainly used throughout this study, except to evaluate pressure drop for which a higher flowrate was used to develop a pressure drop curve across a larger velocity margin.

Maximum velocities were measured in inches of column height (WC) with a total pressure pitot tube connected to the high side of the manometer and a static pressure pitot tube connected to the low side. Hence, the manometer displays the difference in total and static pressure which is the dynamic pressure. A liquid with a specific gravity of 0.826 is used in the manometer, hence the conversion from the column height to pressure can be obtained using Bernoulli's equation:

$$P = \rho_l g h \tag{13}$$

Here, P is the pressure in Pa, ρ_l is the density of the manometer liquid in kg/m^3, h is the height displayed in the manometer in meters and g is the gravitational acceleration (9.81 m/s^2). The obtained data from the manometer is in liquid inches, which is converted to meters and then to

pascals using equation (13). The pressure is then converted to velocity by the relation of pressure-velocity in Bernoulli's equation:

$$Vmax = \sqrt{\frac{2*P}{\rho_a}} \tag{14}$$

Here, ρ_a is the average density of the air in the dehumidifier which for this study is calculated using equation (7) at the average inlet and outlet temperatures. The average density is calculated by adding the inlet and outlet densities and dividing by two. There is less than 10% change in density from the inlet and outlet conditions of the air so an average approximation can provide close enough values to calculate the flowrate.

The average velocities for this study are all between 0.7 – 1.2 m/s and based on the hydraulic diameter of the duct and the properties of the air the Reynolds numbers range between 3000 – 5300. To simplify the use of equations, and since the flow is outside of the laminar regime (Re < 2200), turbulent flow equations were used for calculations that include flowrate and pressure drop. Equation (15) and (16) are used to obtain the average velocity from the measured maximum velocity as shown in [72].

$$\frac{1}{f^{1/2}} = -2.0\, log\left(\frac{2.51}{Re\, f^{1/2}}\right) \tag{15}$$

$$u_{avg} = \frac{1}{(1+1.3f^{1/2})}\bar{u}_{max} \tag{16}$$

For turbulent flow, an iterative process needs to be done to obtain the average velocity from a given maximum velocity. Equations (15) and (16) are used starting with a guessed friction factor value until the iteration converges to the true value of f. Hence, for this study, the air flow rate was calculated indirectly from the maximum velocity measurements of the manometer. The

maximum velocity measurements provided by the manometer converted to average velocity and mas flowrate ate shown in table 3 below.

Table 3: Average velocities and flowrates used for this study.

Avg Velocity (m/s)	Flowrate (kg/s)
0.70	0.0040
1.00	0.0060
1.20	0.0070

4.2 Effect of poly-cotton strings on dehumidifier

For this section, the effect of parallel poly-cotton strings (75% Polyester and 25% cotton) along the axial direction of the dehumidifier is studied. Eleven Stainless Steel strips of 1.2 mm thickness were used on each side of the duct to tie in the strings with enough tension to ensure their parallelism throughout the testing. Figure 16 shows a picture of the inlet of the duct with 120 strings installed.

Figure 16: Picture of inlet of dehumidifier duct with 120 strings installed.

The dehumidifier duct was first tested at an inclination of 5 degrees from the horizontal to test its performance at a low inclination angle just enough to allow the condensed water to run down the dehumidifier to be collected. The testing in this section was performed at four different number of strings (N); 120, 65, 33 and 0. Figure 17 shows the results in temperature drop along the dehumidifier duct as N increases from 0 to 120 strings at a fixed velocity of 0.7 m/s. Since temperature data were obtained only at the inlet (x=0m) and the outlet (x=1.9m) of the dehumidifier duct, a linear connection between the two data points is made as an approximation for visualization purpose.

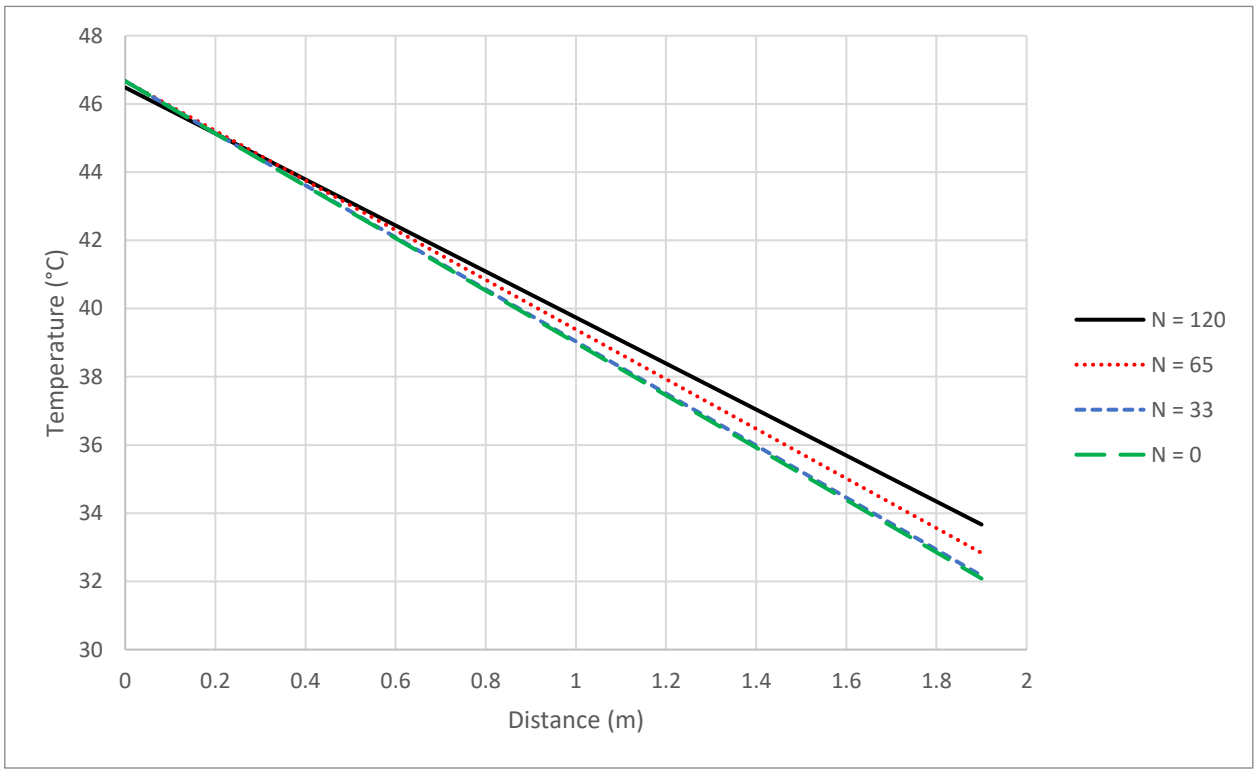

Figure 17: Temperature drop along the axial direction of dehumidifier at different number of poly-cotton strings. Testing performed at a fixed velocity and duct inclination of 0.7 m/s and 5° respectively.

The testing design used in this study allows for a maximum inlet temperature at the dehumidifier of ≈ 46.7 ℃ due to limitations on the humidifier components. Therefore, all data throughout this study is obtained at this inlet temperature. Since the rate of water production is directly related to the temperature change across the dehumidifier, the axial temperature drop is largely discussed to compare the effectiveness of the dehumidifier. Figure 17 clearly shows the trend of temperature drop in the dehumidifier as N increases. Contrary to previous studies that use vertical bundles of parallel strings, the temperature drop decreases as the number of string increases. The temperature drop between the duct configurations of 0 and 33 strings is insignificant, however, as the number of strings increases to 120, the temperature drop decreases by 1.5 °C as compared to the 0-string configuration. The highest temperature drop is achieved with no strings with a total drop of 14.6 °C.

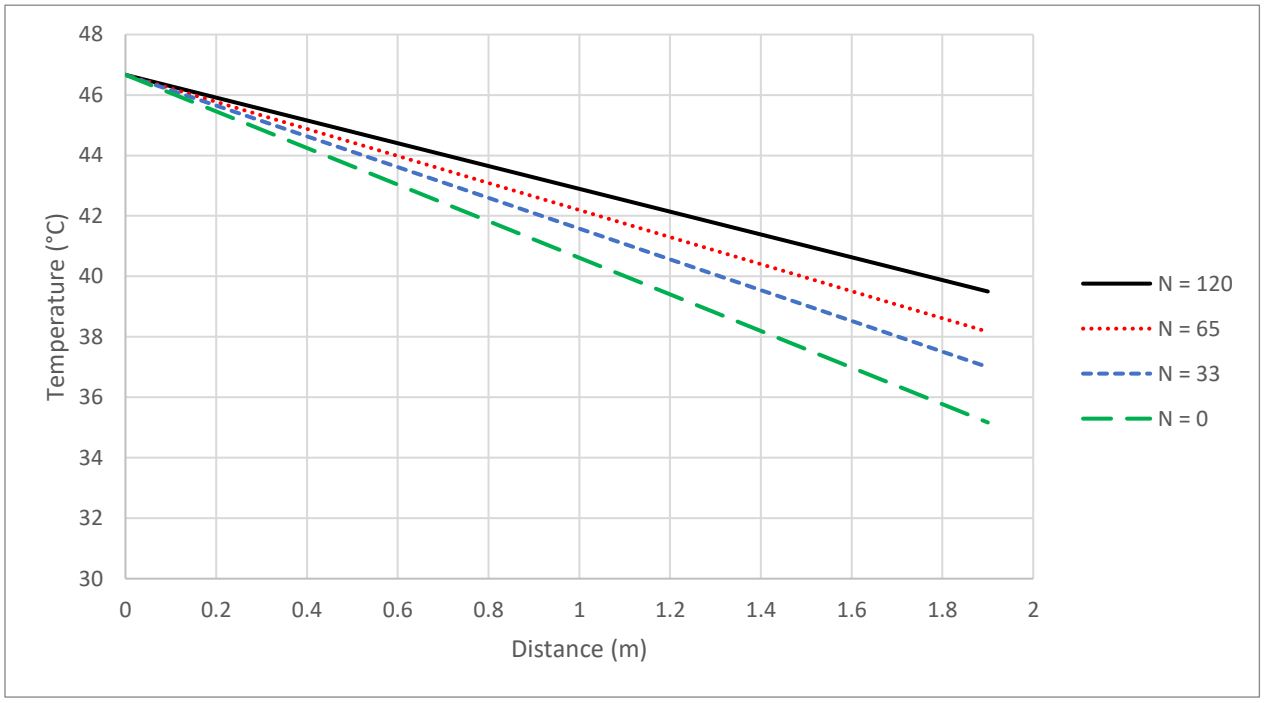

Figure 18: Temperature drop along the axial direction of dehumidifier at different number of poly-cotton strings. Testing performed at a fixed velocity and duct inclination of 1.0 m/s and 5 degrees respectively.

Further testing was made at an increased flow rate to compare, the results are illustrated in Figure 18. At this increased flowrate the overall trend is even more noticeable than the testing at 0.7 m/s. A larger difference in temperature drop of 4.3 °C is observed between the test with 0 and 120 strings. The efficiency of the dehumidifier to cool down the air seems to be compromised as the number of strings increase, causing a decrease in temperature drop. The same trend is clear at the two tested flowrates which provide enough information to safely assume that this will be the case at any similar flow rate.

The rate of water production was also quantified by dividing the total water produced by the testing time. Figure 17 shows the comparison in water production in g/min at the two testing velocities 0.7 and 1.0 m/s. The same trend as the temperature drop is observed, the rate of water production decreases as N increases.

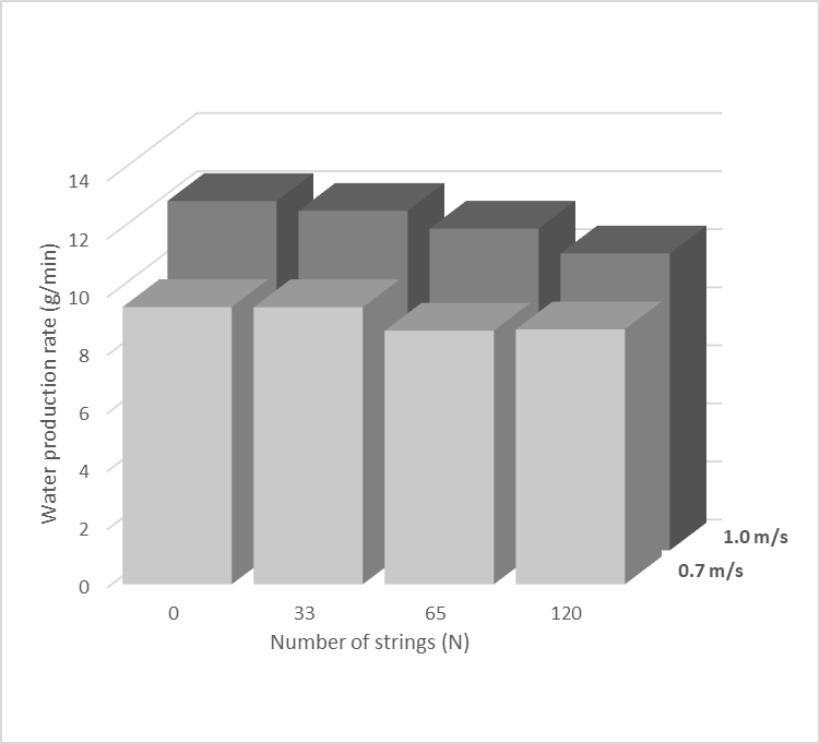

Figure 19: Freshwater production achieved at two different flow velocities, 0.7 and 1.0 m/s as the number of strings increases.

The temperature and water production data obtained with the poly-cotton strings points to the same conclusion; as the number of strings increases, the efficiency of the dehumidifier decreases causing a lower temperature drop across the dehumidifier and consequently, reducing the amount of freshwater produced. To verify the experimental data obtained, the simple control volume approach shown in Figure 6 was analyzed with the mass and energy balance equations. Equation (2) was used to determine the amount of water produced at the known flowrate and temperature drop to compare to the experimental data.

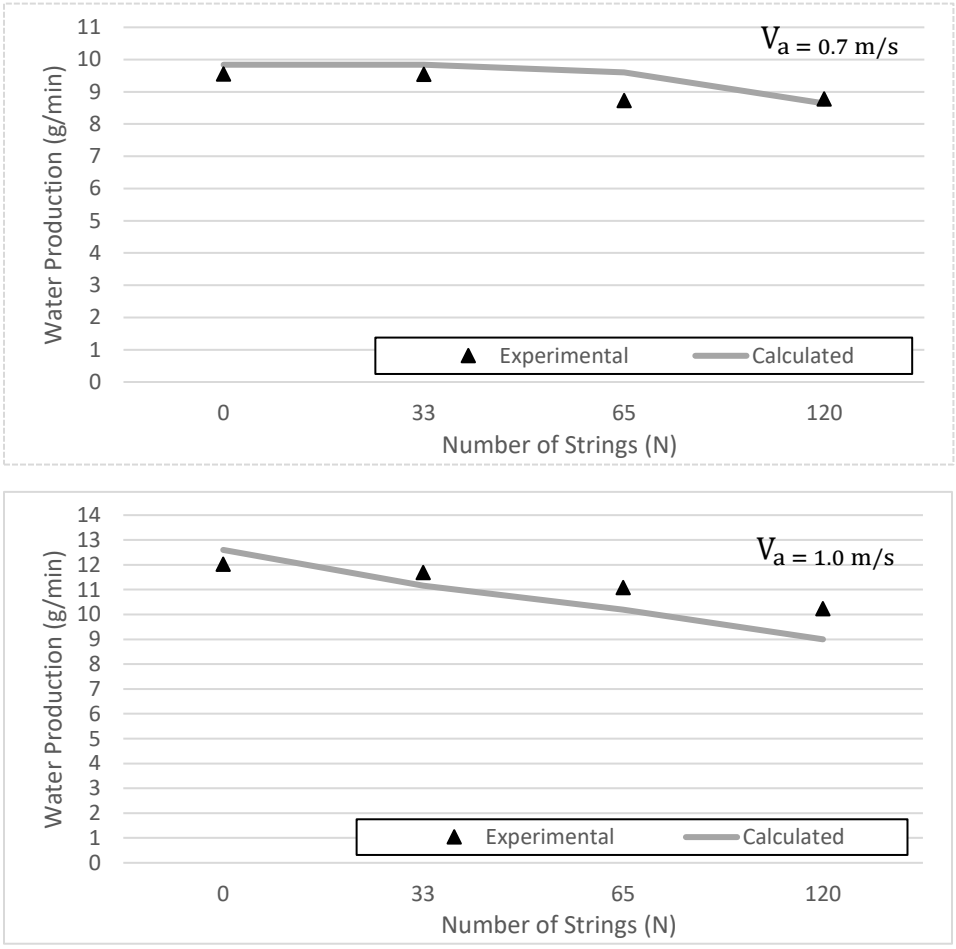

Figure 20: Comparison of experimental and calculated water production as the number of strings increases. Average velocity of air 0.7 m/s (top) and 1.0 m/s (bottom).

Figure 20 shows the comparison between the experimental and calculated data at the two tested flow rates. Variations in air flow rate were shown to be insignificant at any number of strings during experimental testing, therefore, flowrate was maintained constant for had calculations. Since flowrate is maintained constant, the only parameter affecting the freshwater production is the change in temperature drop across the dehumidifier. Since the cooling and dehumidification occurs at approximately 100% RH, to increase the freshwater production the temperature drop needs to increase which is proportional to the humidity ratio (grams of water vapor over grams of dry air) of the air. As the temperature drops, saturated air loses its ability to hold vapor molecules and condensation occurs, hence, an increased temperature drop is directly related to an increased water production. The calculated data obtained from the mass conservation equation of the dehumidifier closely confirms the experimental data obtained of freshwater production with an average error 6.04% and a maximum error of 13.60%. The maximum rate of water production was achieved with no strings present at a rate of 12.03 g/min. This configuration yields a freshwater production of 0.722 l/hour or 17.3 l/day which is achieved at a mass flowrate of 0.006 kg/s (1.0 m/s) of humid air.

As mentioned before, an important parameter to determine the overall efficiency of dehumidification systems is the total pressure losses across the system. The pressure loss across the dehumidifier was measured by using two static pressure pitot tubes located 0.9 meter away from the inlet of the dehumidifier to allow the air flow to develop and obtain accurate readings. The pitot tubes were located 0.85 meter apart from each other as shown in Figure 15. Figure 21 shows the pressure drop as a function of velocity for all string configurations (N=0, N=33, N=65, N=120). The overall trend clearly shows that the pressure drop increases as the flow increases which is the expected outcome since pressure drop is a related to the square of the velocity for

turbulent flow (equation 10). Additionally, as N increases, the pressure drop shift upward due to the increased surface area and friction for the air flow. Pressure drop values obtained in this study are lower than the results obtained by Sadeghpour et al. [35] in which they show that the numerical simulation and experimental results at 0.75 m/s and 52 strings result in a pressure drop of 1.3 Pa/m. The closest comparable value in this study may be obtained from the pressure drop at 0.7 m/s with 65 strings which resulted in a pressure drop of 0.54 Pa/m.

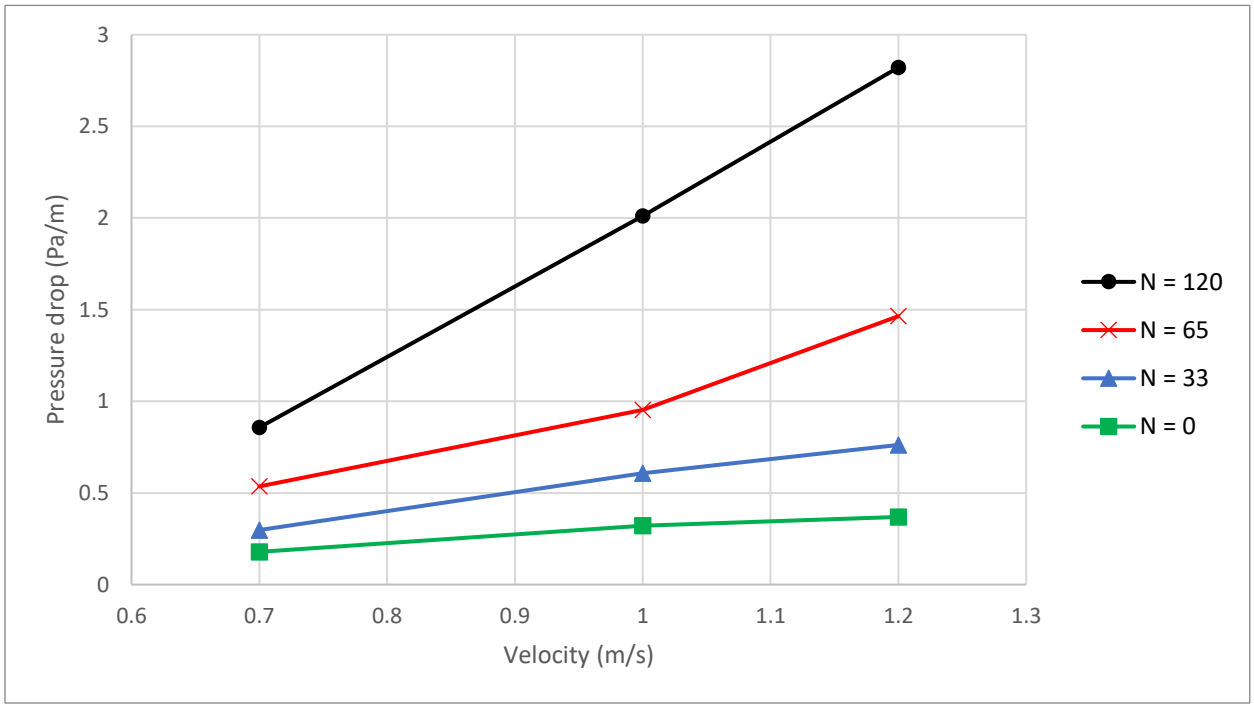

Figure 21: Pressure drop over length (Pa/m) along the axial length of dehumidifier.

The lower pressure drop values obtained in this study are reasonable considering that for this study the flow path for the air is nearly horizontal instead of vertical, hence, reducing the pressure drop due to gravity. Additionally, since water droplets in the strings are forming due to condensation and no liquid is being injected on the strings, there is a reduction in counterflowing friction between the liquid and gas streams, and a reduction in pressure drop due to condensation. A simple pressure drop calculation based on equation (10) was performed to

compare the experimental data. Since the cross-sectional area of the duct is a square, and the strings add a higher contact surface, a hydraulic diameter as a function of cross sectional area and surface diameter can be calculated using the correlation [73]:

$$D_h = 4\frac{A}{P_h} \tag{17}$$

The comparison of the results from the calculated values and the experimental data are shown in Figure 22. The calculations can predict the pressure drop with an average error of 7% for 65<N<0. The configuration with 120 strings presents 30% higher pressure drop in the experimental data than the calculated values, hence, the equations are not accurate to predict pressure drop at this highly dense string configuration. The calculations agree with the experimental data with enough accuracy to validate the experimental results obtained.

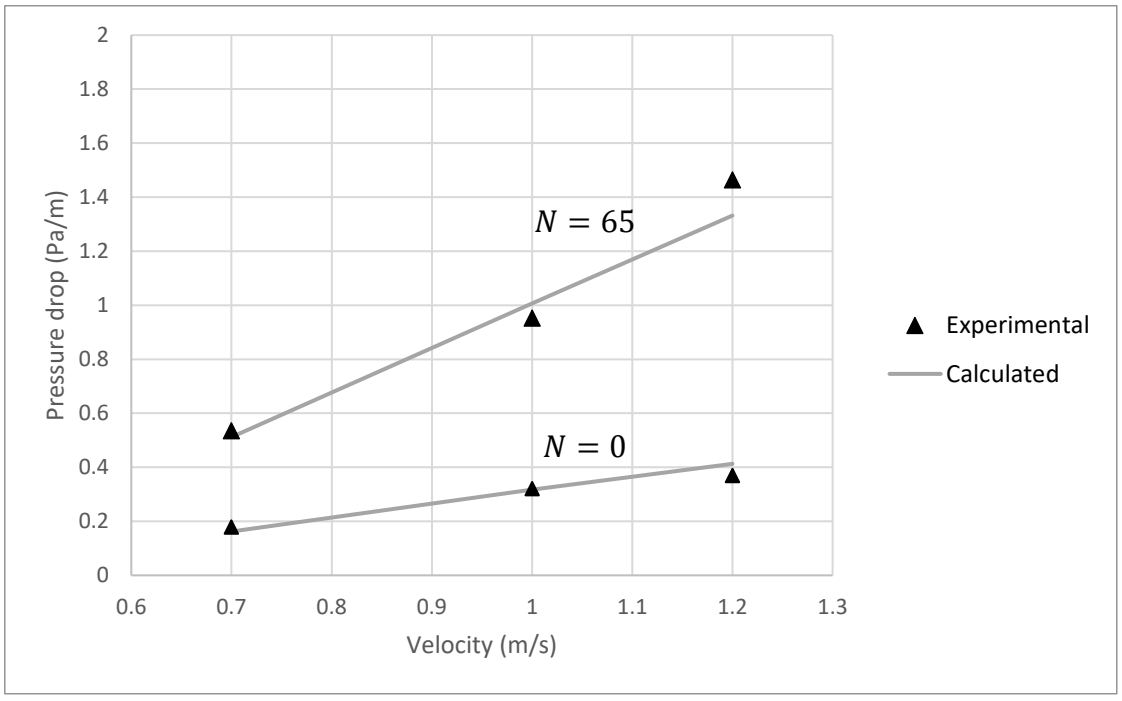

Figure 22: Experimental and calculated pressure drop across dehumidifier.

The data obtained and presented in Figures 17, 18 and 19 suggest that the presence of poly-cotton strings at an inclination of 5 degrees, decrease the capability of the dehumidifier to cool down the air and produce fresh water. To have a visual understanding of the effect of parallel strings inside the dehumidifier, three observation windows were made on the duct near the inlet, the middle, and the outlet as shown in Figure 23. The observation windows were sealed with ASTM C920 silicone to prevent leakage during testing.

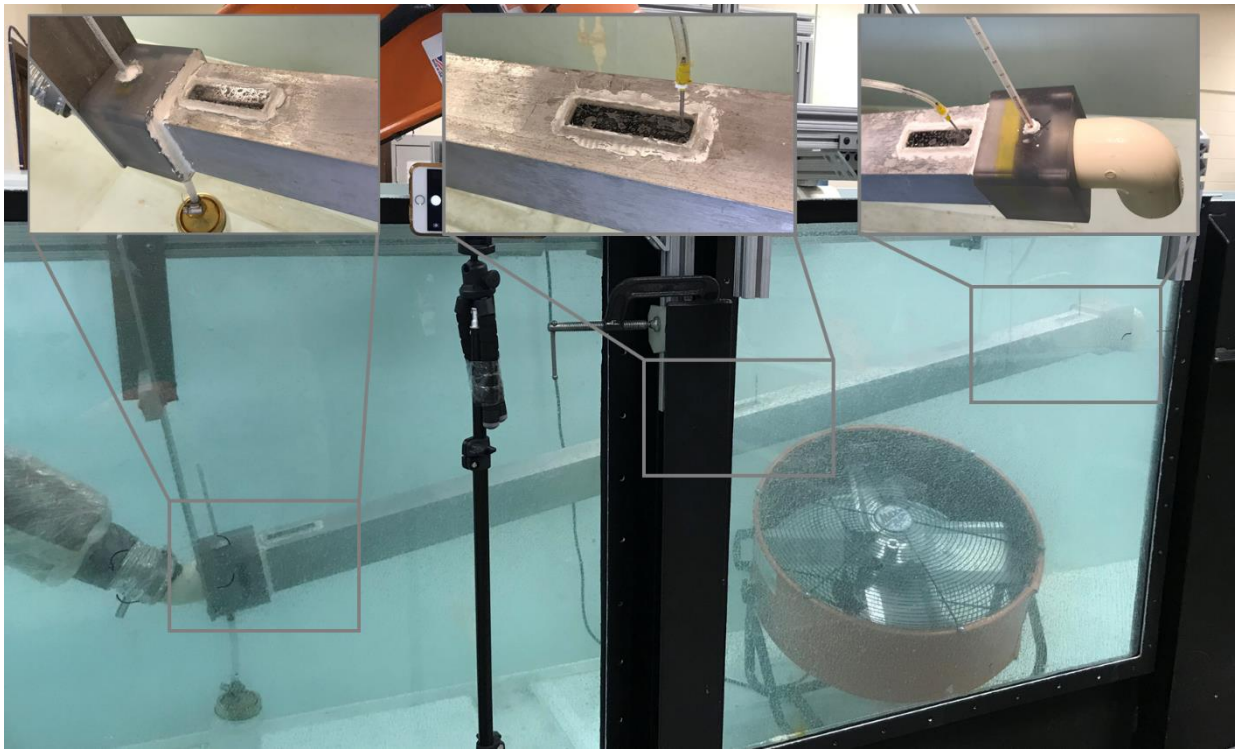

Figure 23: Location of observation windows in dehumidifier. The holes for the windows are 19 x 76 mm.

The proposed hypothesis for this testing was based on the assumption that strings would form water droplets similar to the strings-of-beads shown in earlier studies due to the condensation and pinning of water molecules to the string surface and the inclination of the strings would cause the droplets to slide down the strings improving heat and mas transfer due to

the counterflow contact of cooler liquid droplets and the incoming hot air. To observe the effect of the strings while humid air was flowing, the windows were carefully removed one at a time during testing for a short period of time. It was clearly observed that the poly-cotton strings did not present a high number of water droplets forming around their circumference, instead, the strings seem to get wet and absorb some water within their fibers. Additionally, the high surface tension between the strings and the water prevents the droplets to slide down the strings at a 5-degree inclination, hence, some droplets form around the strings but they stay static until their weight cause them to fall to the bottom of the duct to be collected. Figure 24 is a picture taken at one of the windows.

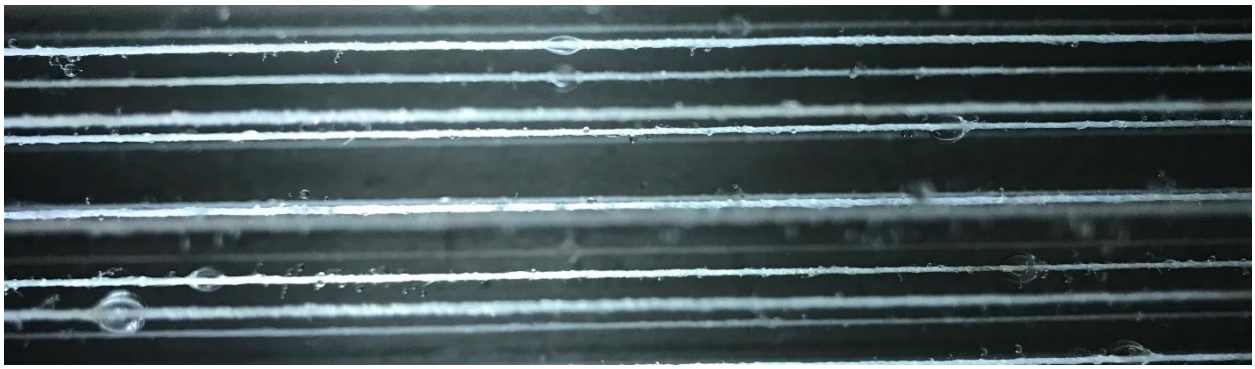

Figure 24: Picture taken after testing the system at 1.0 m/s with 65 poly-cotton strings with dehumidifier inclined at 5 degrees.

4.3 Changing string material

The tests discussed in this section target to explain the effect that parallel strings of various materials have on the condensation of passing humid air. Previous studies that used a bundle of parallel strings for heat and mass transfer have tested various materials such as PTFE, stainless steel, glass, and cotton [35,43]. Glass is a highly wettable material and has been studied to achieve full wetting for applications in which low-surface energy liquids with high viscosities

were used, such as silicone oil. It was found that the flow behavior of a liquid in a wire is primarily dependent on its diameter, liquid wettability, and flowrate of the liquid. Water is a high surface energy liquid with low viscosity and the influence of the surface tension of the wire is more pronounced. For this reason, other studies have used cotton strings to increase the surface tension. Additionally, cotton strings showed that the fibrous structures can absorb water acting as super-hydrophilic strings. The hydrophilicity of the polycotton strings promotes FWC on the surface of the string that may be beneficial for water bead sliding when strings are fully wet since the water film can act as a lubricant to facilitate the sliding of water beads.

To compare the data obtained using the polycotton strings, further testing was done using the 0.33 mm nylon fishing line and 0.58 mm zinc-galvanized steel wire. For this testing, the number of strings and angle of the duct were fixed at N=65 and 5° respectively. Temperature drop, water production and pressure drop are compared between the three string materials and the duct with no strings.

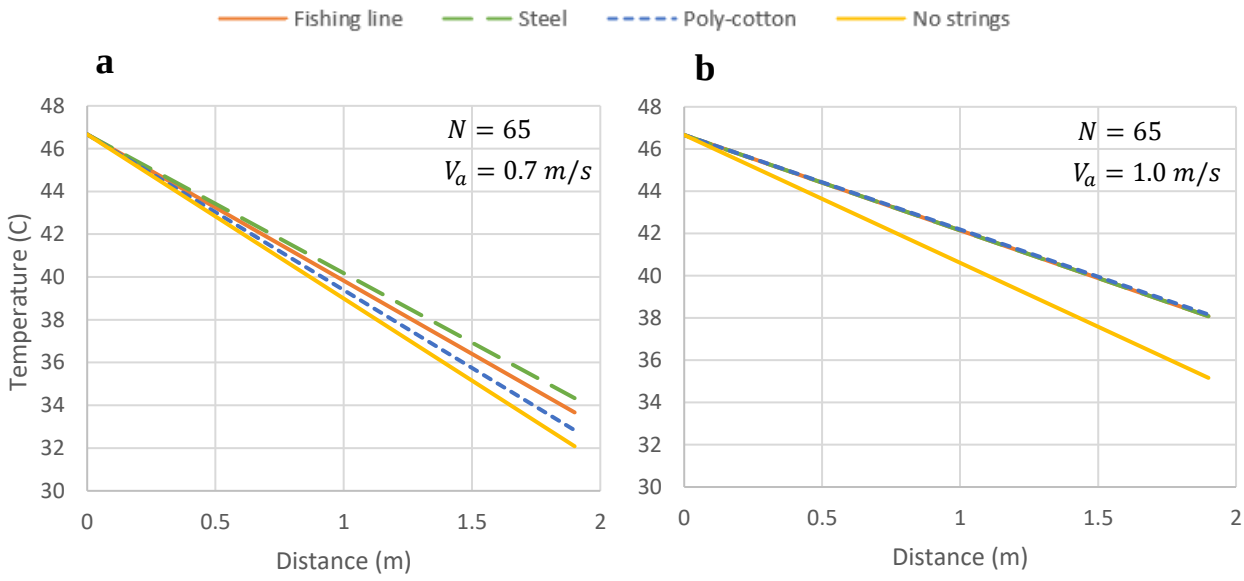

Figure 25: Temperature drop along the axial direction of dehumidifier at a) 0.7 m/s and b) 1.0 m/s. Dehumidifier angle is 5 degrees.

Figure 25 shows the temperature drop across the dehumidifier at the two tested velocities. The string material appears to be more influential on the temperature drop at the lower flow rate as shown in Figure 25a with steel showing the worst performance. Figure 25b (testing at 1.0 m/s) suggests that, at that increased flow, the string material becomes less influential showing the same temperature drop across the system with any string material (the temperature drop line of all string materials is overlapped). At both flow rates, however, the best temperature drop is achieved with the dehumidifier with no strings. These findings further support the data obtained with the polycotton strings. The water production also suggests that the presence of the string array decreases the efficiency of the dehumidifier and water production. Figure 26 shows the comparison in water production.

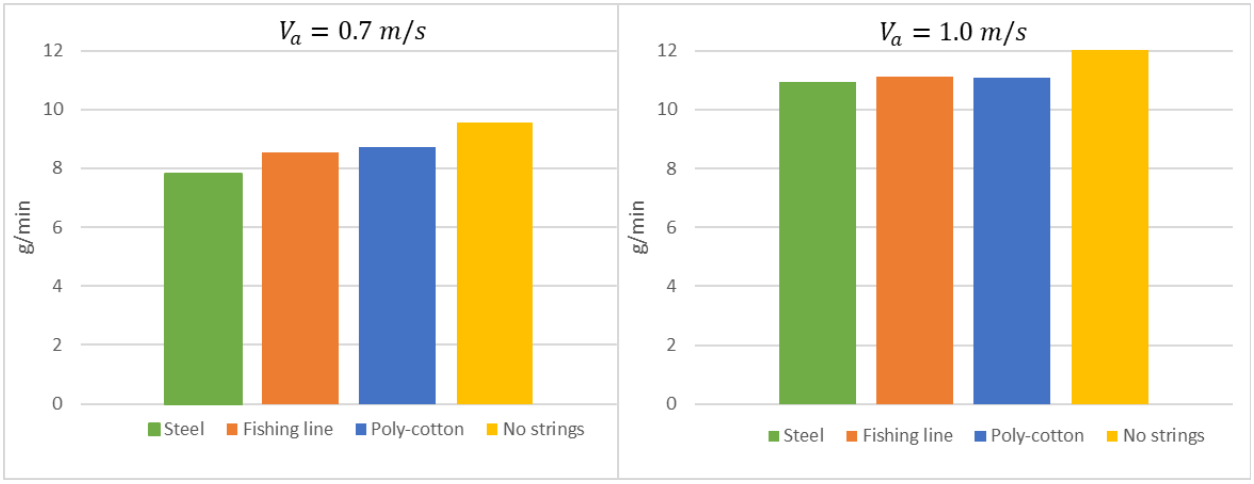

Figure 26: Water production of all string materials at N = 65 for both air flow velocities.

The water production follows the same trend shown in the temperature drop with the steel wire showing the lowest performance in water production for both air velocities and the no-string configuration the highest. Interestingly, the water production presents a similar behavior to the temperature drop as the air velocity increases to 1.0 m/s. The water production shows a staggered

increase as the string material changes at 0.7 m/s. However, at 1.0 m/s the water production is seemingly constant for all string materials, similar to the temperature drop at this flow velocity.

The changes in the pressure drop as a function of air velocity are sown in Figure 27. For all string materials at N=65 the pressure drop increases significantly as the air velocity increases. The fishing line and poly-cotton string configurations show a similar pressure drop, while the steel wire is higher as the velocity increases.

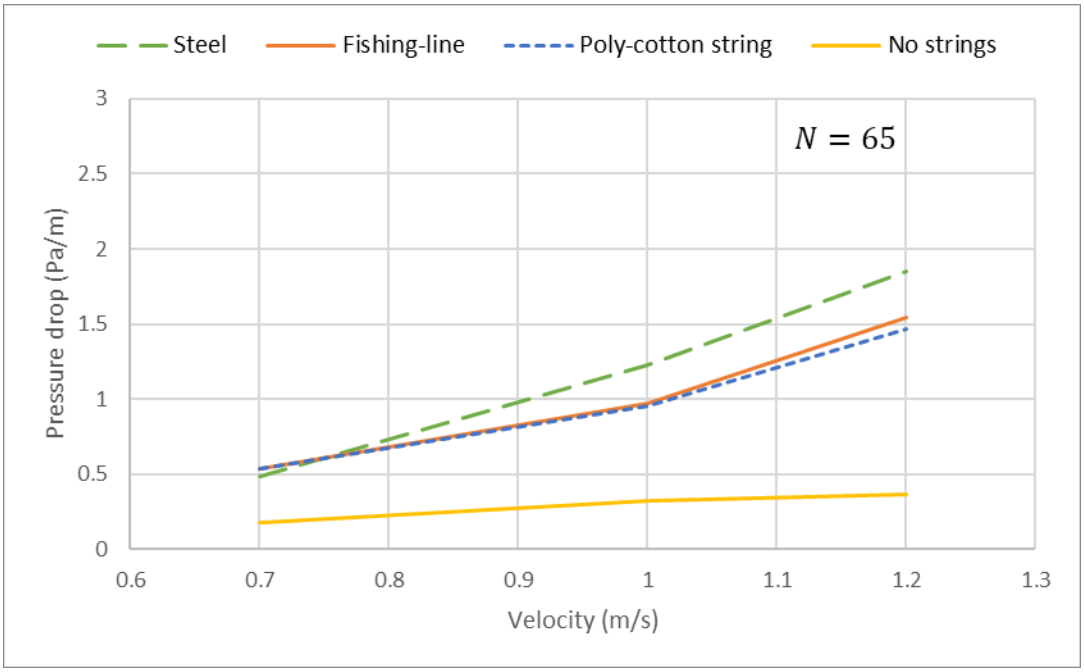

Figure 27: Pressure drop as a function of velocity for all string materials at N=65.

The increase in pressure drop with the steel wire configuration may be attributed to the crooked nature of the wires as they are installed inside the dehumidifier. The non-elastic characteristic of the wire does not allow a perfectly stretched cylindrical surface on the axial direction of the duct, hence, flow path of the air is not as consistent as the other string materials. Figure 28 shows the pictures taken at the observation windows to compare the water bead formation for each string (or wire) material.

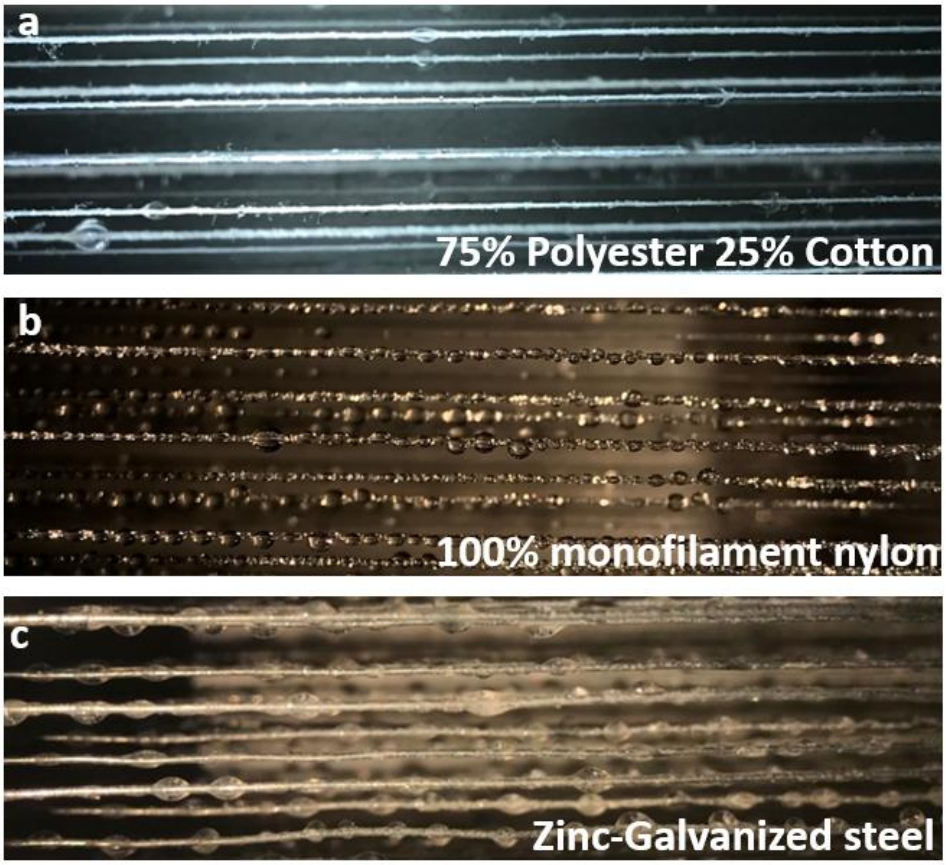

Figure 28: Pictures taken at the observation windows after reaching steady temperatures at the dehumidifier with a) poly-cotton strings (d = 0.55mm), b) fishing line (d = 0.33mm), and c) steel wire (d = 0.58mm). Pictures taken at an inclination angle of 5 degrees.

The string-of-beads effect is observed at varying patterns with the material change. The fishing line and steel wire present a much higher count of water droplets compared to the poly-cotton string. This difference seems to be caused by the absorbance of the poly-cotton strings that create a hydrophilic surface promoting mainly FWC on its surface. The hydrophobicity of the material and diameter also influences the size and shape of the water beads. As observed in the pictures in Figure 28, the fishing line can produce many more small beads around its circumference. It appears that DWC is dominant in the polymeric material of the fishing line while FWC is more dominant on the poly-cotton strings. The metal wire, on the other hand,

forms similar-shaped beads as the polycotton strings showing a hydrophilic surface, but the non-absorbent steel is able to form many more water beads as compared to the polycotton. For any material however, the same behavior is observed in terms of water bead movement; the water beads are static on the surface of the string (or wire) at this inclination angle.

4.4 Changing the dehumidifier angle

The testing previously discussed was performed at a fixed dehumidifier angle of 5 degrees from the horizontal. The small angle allows for a semi-horizontal position of the long duct that allows some of the produced freshwater to flow back to the water-collecting jar. However, the experimental data and observations of the strings show no movement of water beads along the strings.

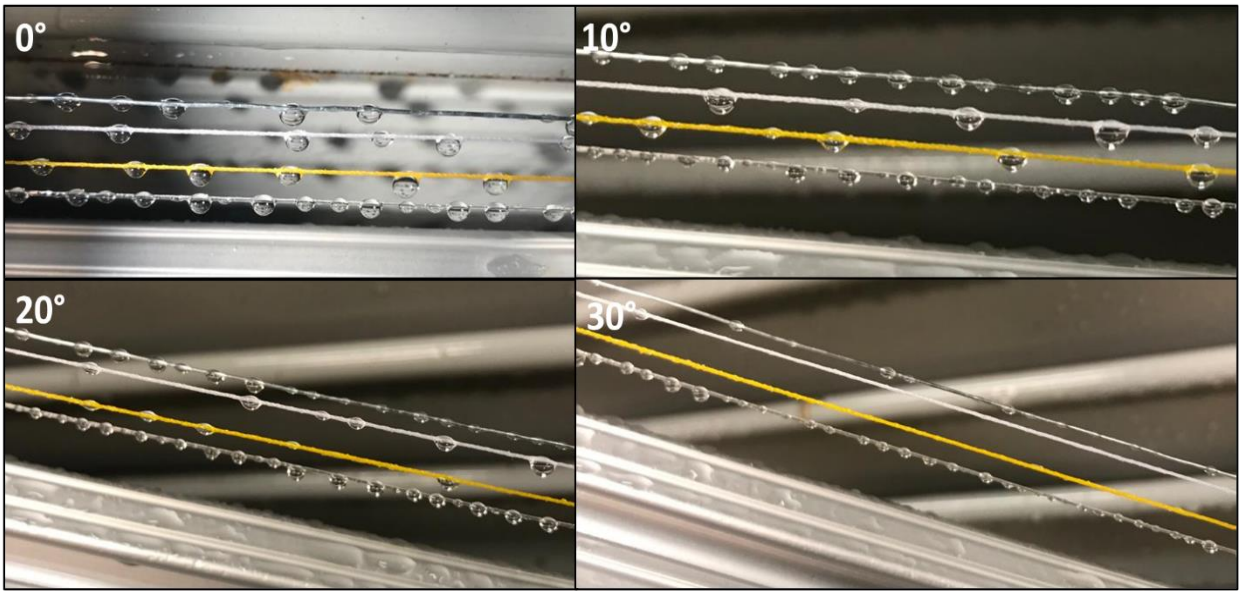

Figure 29: Water bead sliding test at angles from 0-30 degrees. The string materials are as follows, starting from the top; Zinc-galvanized steel wire, 75% polyester 25% cotton, 100% polyester, and monofilament nylon.

To further understand the behavior of the water droplets along the inclined strings, a simple test was performed with all the selected string materials tied to a 2-meter-long beam. The strings were sprayed with ambient temperature water until fully saturated to form the string-of-beads. The beam was then inclined at various angles to observe the behavior of the water droplets along the strings. Figure 29 shows the pictures taken during the test. It was observed that the water bead formation in all string materials is similar when fully saturated with water at the horizontal position (0-degree inclination). However, as the inclination angle increases, the water droplets start to slide down the strings. At the 30-degree inclination the polycotton and polyester strings showed the best water bead sliding. Water beads also started to slide down the steel wire at this angle, however, it was also observed that due to the non-elastic nature of the wire, a low-tension installation allowed the wire to vibrate considerably more than the other strings.

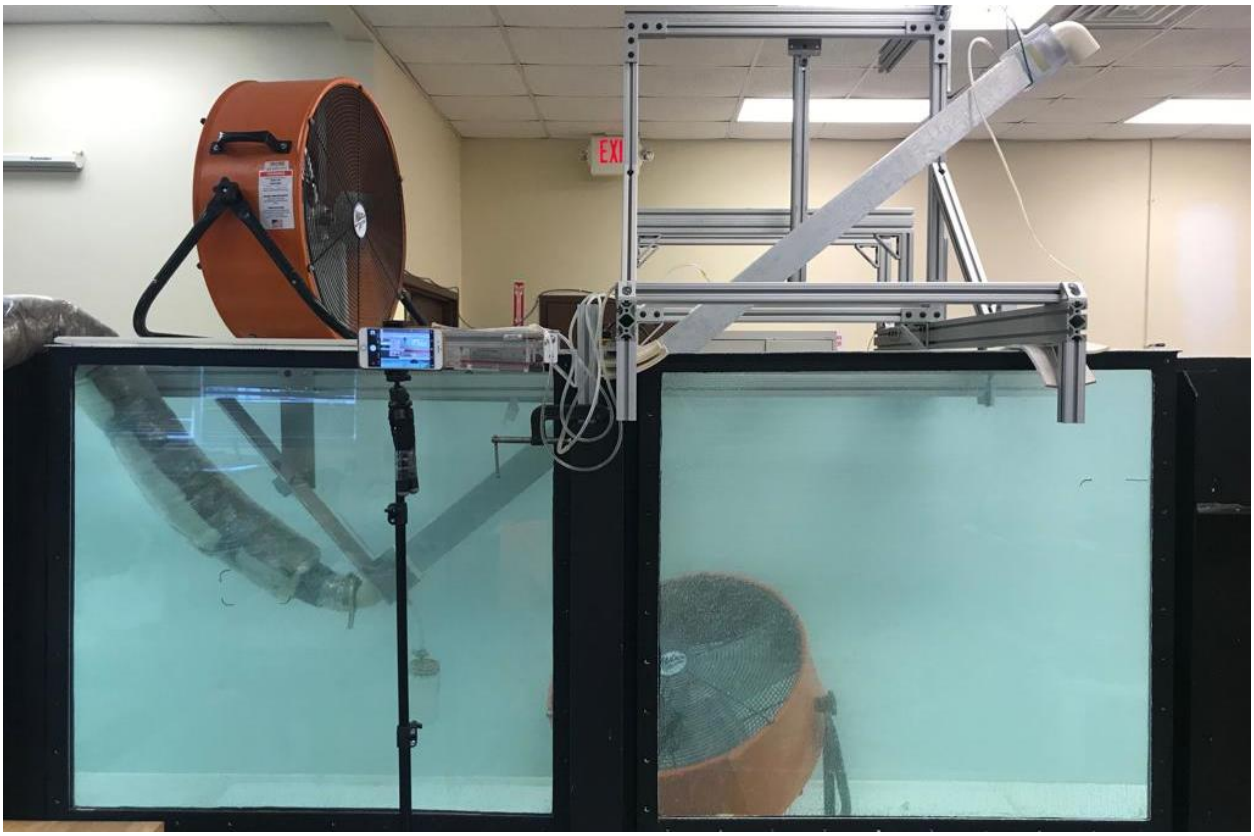

Figure 30: Picture of the dehumidifier setup at a 40-degree inclination angle.

These vibrations seem to improve the water bead motion along the wire. The fishing string showed the best water bead number with almost three times more bead formation than the other strings, but the surface tension is high, not allowing the water droplets to slide at any inclination angle. These findings lead to further testing but at an increased inclination angle to promote better water bead sliding and compare how this affects the effectiveness of the dehumidifier. An inclination angle of 40 degrees was fixed for the testing discussed in this section. For this testing the same air flow rates were used (0.7 and 1.0 m/s), and the number of strings was fixed to N = 65. Ambient conditions were held constant with the same rate of water spraying on the outer walls of the duct and the fans at similar position above and under the dehumidifier as seen in Figure 30.

The temperature drop comparison between the 5- and 40-degree testing is shown in Figure 31 for all string materials and the dehumidifier with no strings. The data obtained at 0.7 m/s shows no significant change in temperature drop between the 5- and 40-degree configurations in all cases. Nevertheless, the 1.0 m /s testing shows a larger difference in temperature drop between the two angles for all string materials. The maximum difference was observed with the polycotton strings with an increase of 1.17 ℃ in temperature drop across the dehumidifier from $\Delta T_5 = 8.53$ ℃ to $\Delta T_{40} = 9.70$ ℃, where the subscripts 5 and 40 represent the inclination angle respectively. This change in temperature drop may be attributed to the increase in water bead sliding observed with the polycotton strings at this increased inclination. The fishing line and steel wire configurations had a negligible change in temperature drop at this increased inclination, similar to the no-string configuration. Therefore, increasing the inclination of the dehumidifier duct only has a significant affect if the string material has low surface tension when fully wetted, allowing the water beads to slide down the thread.

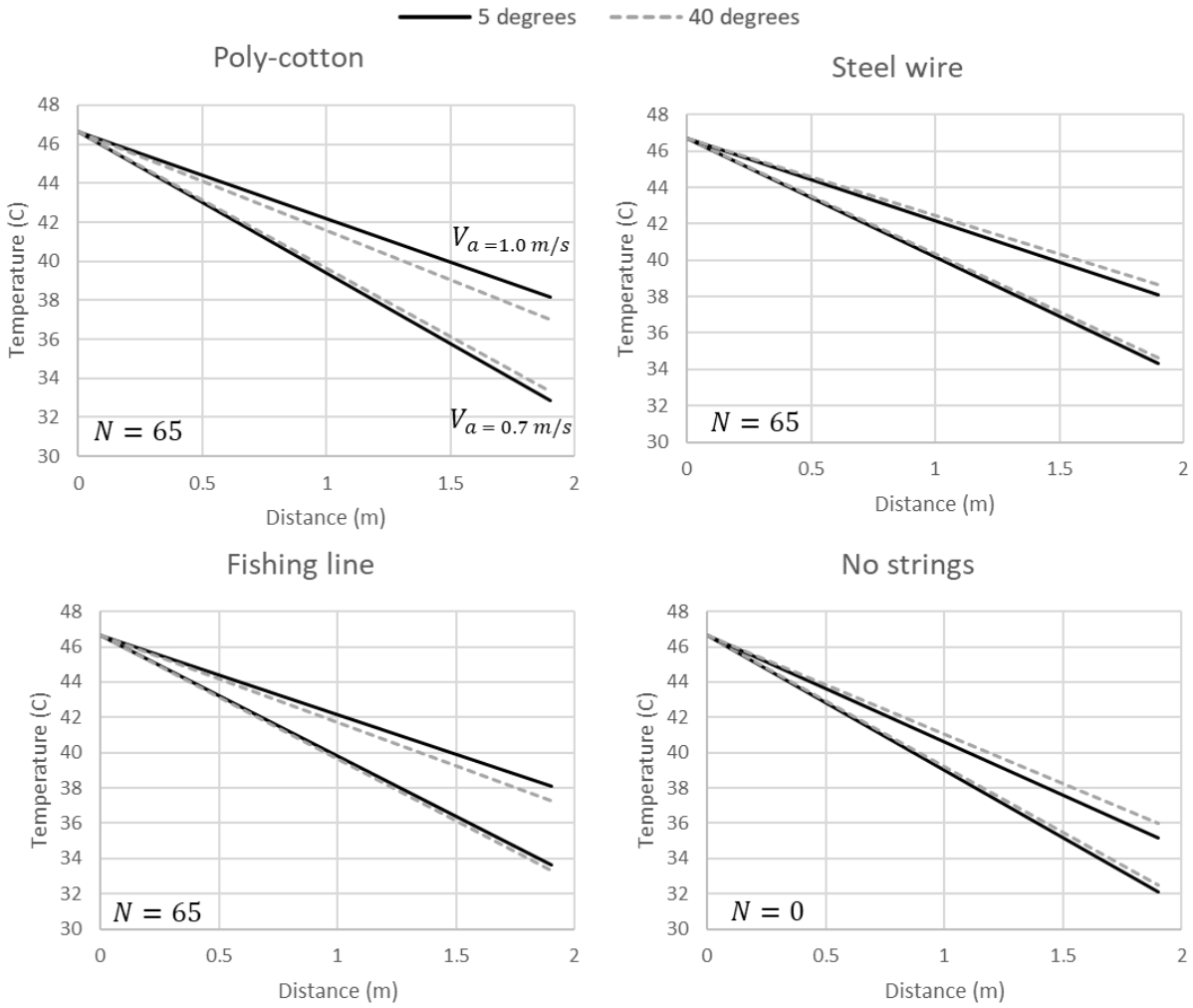

Figure 31: Temperature drop comparison at 5- and 40- degree dehumidifier inclination.

This slight temperature drop difference provides a higher effectiveness for the dehumidifier using poly-cottons strings compared to the other string materials. The effectiveness of the different string configurations is compared in Figure 32 for both testing angles at an air flow rate of 0.7 m/s (Figure 32a) and 1.0 m/s (Figure 32b). The effectiveness is calculated based on the ideal condition in which the outlet air exits the dehumidifier at ambient temperature (22 °C) as discussed for equation (12).

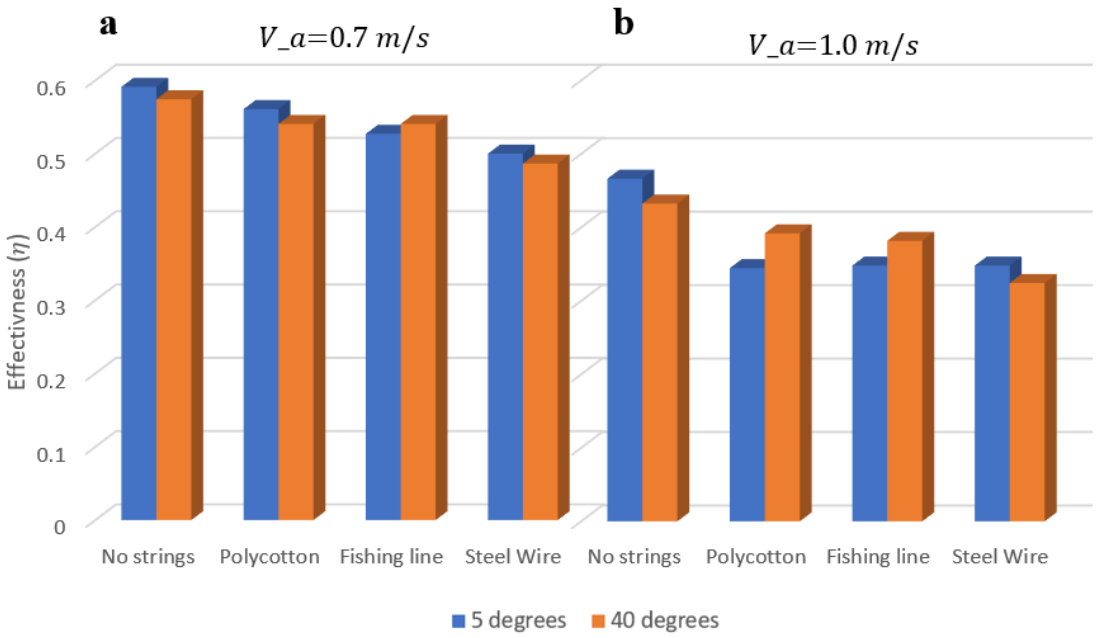

Figure 32: Effectives of dehumidifier with different string materials (N = 65) at a) 0.7 m/s and b) 1.0 m/s.

The effectiveness of the dehumidifier to cool down the air drops significantly as the air flow rate increases. This is expected since the time that the air spends in the duct decreases as the velocity increases, hence, decreasing the heat transfer time. The higher effectiveness value is achieved by the duct with no strings at air velocity of 0.7 m/s, and the angle at 5 degrees, with $\varepsilon = 59\%$. Observation inside the duct after each test verified the same water bead behavior previously observed by spraying the strings. The pictures through the observation windows are show in Figure 33. Figure 33b and 33c show that the steel wire and fishing line formed many water beads but even at this inclination, the same static behavior prevailed not allowing them to slide down the dehumidifier to create direct contact heat transfer and to be collected. The polycottons strings on the other hand, did not show nearly any water beads on the strings as compared to the 5-degree pictures as shown in Figure 28a, which mean that the water droplets are sliding back to be collected. This may be the reason for the increased temperature drop at 40

degrees as compared to the 5-degree testing. However, the temperature drop is not as pronounced as expected. This could be caused by two main reasons; 1) the water bead formation on the poly-cotton strings is not as numerous as the other string materials. As seen in Figure 28a, only a few droplets of enough size to be able to slide, form around the strings.

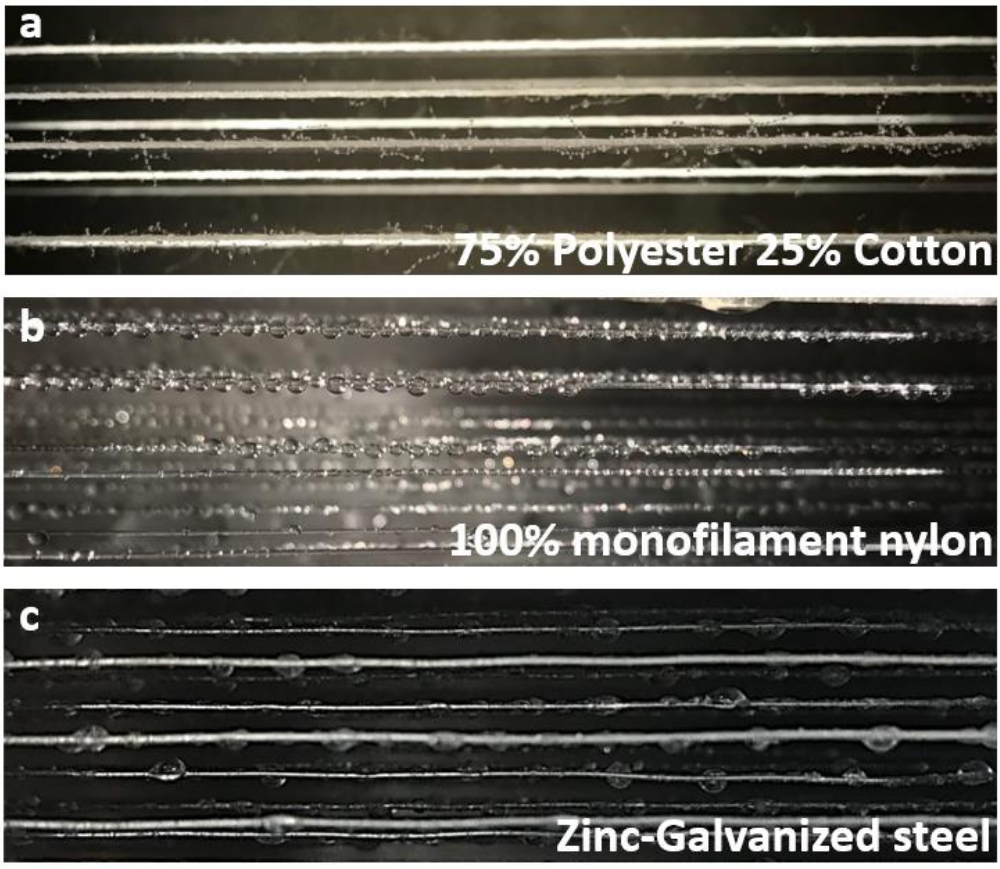

Figure 33: Pictures taken at the observation windows after reaching steady temperatures at the dehumidifier with a) poly-cotton strings (d = 0.55mm), b) fishing line (d = 0.33mm), and c) steel wire (d = 0.58mm). Pictures taken at an inclination angle of 5 degrees.

The other string materials are much better in forming water beads, but for these strings, the beads do not slide back even at high inclination angles. Additionally, 2) the temperature drop across the dehumidifier is not big enough (i.e. $\Delta T_{40} = 9.70$ ℃ at 1.0 m/s for the polycotton

strings) so even if the few water beads that form with the polycotton string slide back the dehumidifier, the temperature difference between the water droplets and the incoming humid air is not enough to make a substantial difference.

The water production rate with the dehumidifier at a 40-degree inclination follows a similar trend shown in the temperature drop and dehumidifier effectiveness. Figure 34a shows the trend of water production with each string material at 1.0 m/s and Figure 34b the percent change between 5- and 40- degree testing. The increased inclination allowed more freshwater to slide down the dehumidifier duct for all string materials and the 0-strings configuration. However, the poly-cotton strings showed the highest improvement in freshwater production with 19.6% increase while the steel wire, fishing line, and no string configurations showed 9.3%, 12.37%, and 11.0% respectively. Again, this increase in freshwater production shows that a higher dehumidifier effectiveness can be achieved if water beads are able to slide down the strings for an increased direct-contact heat transfer with the incoming air.

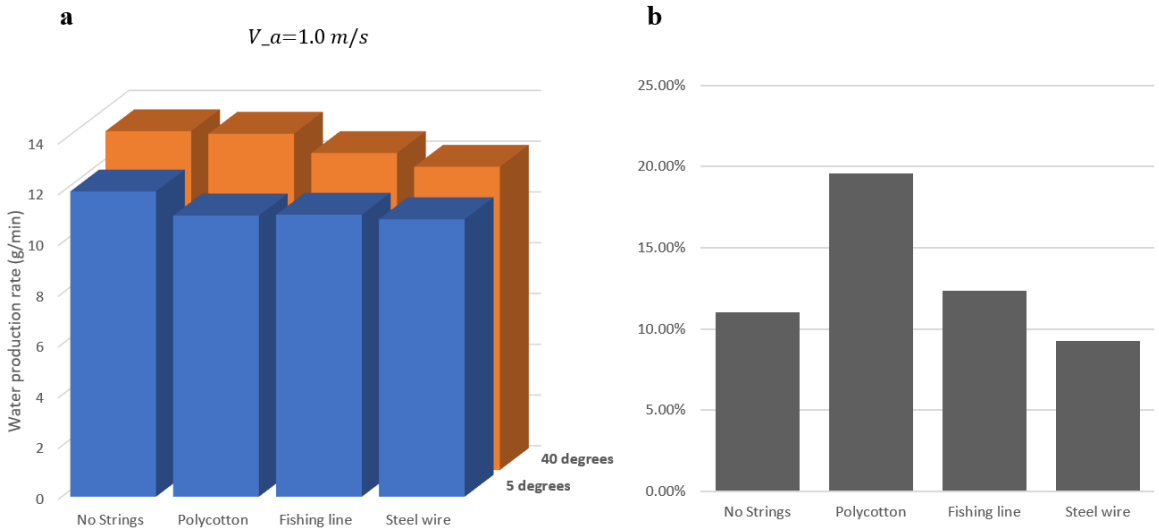

Figure 34: a) Freshwater production comparison at 5- and 40-degree dehumidifier inclination. b) Percent increase in water production.

The increase in water production with the polycotton strings agrees with the increase in temperature drop and efficiency at this increased inclination angle. The polycotton strings also showed the best water bead sliding at this angle improving the amount of water that is collected. However, the overall effectiveness is still lower than the configuration with no strings as seen in Figure 32. This decrease in temperature drop (and effectiveness) in the dehumidifier with any string material, seems to be caused by the wetting and formation of static water droplets on their surface. The water droplets do not slide back on the strings at a high enough rate to provide direct contact heat transfer with the incoming hot-humid air, instead, their static nature seems to interfere with the flow and decrease the efficiency of heat transfer of the air.

Figure 35: Picture of wetted polycotton strings inside the dehumidifier.

The difference in temperature drop at 1.0 m/s between the polycotton strings and the no-string configuration is 1 °C, nevertheless, the difference in water production is barely noticeable with a difference of 0.1 g/min. These results may be caused because the strings provide a higher surface area that helps improve condensation, but they don't provide enough water beads sliding

down to improve direct contact heat transfer. Additionally, the highly pilling nature of the polycottons strings retains much more water in form of small droplets as seen in a picture taken from another angle in Figure 35. The highly fibrous nature of the polycotton strings traps many small droplets and consequently, spite of the fact that some beads of enough size form and slide on the strings, seems that the majority of the surface condensation happens on these small fibers and stay static.

CHAPTER V

CONCLUSIONS AND FUTURE WORK

5.1 Summary and conclusions

A dehumidifier for ocean-based humidification-dehumidification (HDH) applications was investigated. For the testing, a functional HDH system was designed, built, and tested in a laboratory setting. The dehumidifier design was developed with the purpose of being practical and low-cost, utilizing only common commercially available materials. The purpose of the investigation was to study the feasibility of taking advantage of the strings-of-beads effect to develop a simultaneous direct- and indirect-contact heat exchanger for cooling and dehumidification at a low pressure drop. Unlike any previous investigations of the strings-of-beads that utilize a controlled injection of liquid on the strings, this study aims to study the feasibility of achieving the enhanced heat and mass transfer that such intrinsic surface bumps provide, by producing the water droplets with the condensation of humid air along the strings and encouraging the water bead movement only by the inclination angle of the strings.

Fourteen commercially available string materials were tested to ensure their ability to retain tension for extended periods of time when exposed to temperature and humidity changes. This is important to retain the parallelism of the bundle of strings and maintain constant conditions inside the dehumidifier. Three string materials were selected for this testing based on their tension-retention performance and contrasting surface properties; polycotton (75%

polyester and 25% cotton), Nylon fishing line (monofilament), and steel wire (zinc-galvanized steel). The experimental work shows that strings of various materials are able to collect enough water vapor to form water beads around their surface (Figure 26), however, the main challenge lies on improving the movement of the formed droplets along the strings to counterflow the incoming hot-humid air. Water is a high surface energy liquid with low viscosity and the influence of the surface tension of the strings is strong, preventing the formed water beads to easily slide down the strings. Testing performed with the dehumidifier at 5 degrees of inclination shows that all string materials form water beads at different extents, nevertheless, for all string materials, a 5-degree inclination is not enough to cause sliding of the water beads. The presence of the strings and the static water droplets showed a negative effect on the effectiveness of the dehumidifier, therefore, decreasing the amount of freshwater produced.

Pressure drop across the dehumidifier is also a very important factor to decrease the overall energy required to move the airflow through the system. For ocean-based HDH desalination systems this is specially important since this technology often requires the use of low energy requiring components, or even no electric components at all. Parallel strings have shown promising results compared to other technologies to reduce pressure drop for heat exchangers. The proposed dehumidifier is no exception and maintained a pressure drop of less than 2.8 Pa/m. Most of the testing was performed with 65 parallel strings that resulted on a pressure drop between 0.53 Pa/m and 0.95 Pa/m for air flow velocities of 0.7 and 1.0 m/s respectively. The use of strings is a promising approach in order to keep a low pressure drop across the dehumidifier.

Further testing showed that at an inclination of 30 degrees, the polycottons strings provided the best water bead sliding along the strings. The steel wire and fishing line proved to

have high surface tension with the water not allowing the water beads to slide along the strings even when completely vertical. It was also observed that introducing vibrations on the steel wire provided enough excitation on the water droplets making it easier for them to slide down the wire. Additional testing was performed at an inclination of 40 degrees to ensure better water bead sliding on the strings. All configurations showed a 9-12% increase in water production except the polycotton strings which resulted in a 19.6% increase. Nevertheless, the effectiveness of the duct with no strings is still higher than any string material. The polycottons strings showed the best water bead sliding and water production only 0.1 g/min less than the duct with no strigs. This small difference may be caused due to the pilling nature of the polycottons strings that absorb and retain many water droplets on its fibers not allowing the condensed water to flow back to be collected. Additionally, the hydrophilic nature of the polycotton material facilitates filmwise condensation (FWC) on its surface, decreasing the amount of water beads that form on the strings. The nylon and steel strings (or wire) provided faster and increased water bead formation.

This study provides an introductory insight into the possibility of using a bundle of parallel strings to promote direct and indirect heat transfer and dehumidification. The small amount of water beads formed on the polycottons strings and the static presence of the same on the nylon and steel materials proved to decrease the effectiveness of the dehumidifier. The increased inclination provided better water bead sliding for the poly-cotton strings which showed increased effectiveness and water production but not enough to enhance the heat transfer. The ideal string material for this application is one which can produce fast and numerous water beads on its surface and at the same time provides a slippery enough surface for the water beads to slide easily at an inclined angle. At the tested air flowrates this system provided a maximum

water production of 19.2 l/day. Further string material testing is required in order to create the ideal conditions of increased condensation and water bead that could provide an enhanced heat transfer at a low pressure drop.

5.2 Future work

The main challenge of this study lies on finding and testing a cost-effective string material, that ideally is commercially available, and can solve the issues of the tested strings of this study; low water bead formation and high-water retention (i.e. polycotton), and no water bead sliding on the inclined strings (i.e. steel wire and nylon fishing line). A superhydrophobic or hydrophilic-slippery [47] material is needed to improve formation and movement of the water droplets along the strings. However, most studied materials that provide this great surface wetting characteristic are custom made with micro/nano structures, or chemical alterations. A more extensive string material testing is necessary to find commercially available materials that can provide these ideal surface conditions.

Additionally, during testing it was observed that the steel wire can provide increased water droplet sliding when the strings vibrate. From all the materials tested, the steel wire showed an increased sensitivity to prolonged vibrations when a small excitement is introduced on the wires (i.e. slightly touching the wires or hitting the walls of the dehumidifier duct). Another option for increased water bead mobility with this material is inducing vibrations on the wires. For ocean-based systems, is possible to take advantage of the wave motion to introduce a simple oscillating-mass mechanism that hits the dehumidifier duct as the mass moves with the wave motion. Further testing is necessary to prove this interesting concept.

At an increased bead formation and mobility, it is also critical to increase the temperature difference between the water beads and the incoming hot-humid air. The static water beads forming at the same temperature of the passing air is not beneficial for the system as proved in this study. An approximate temperature drop of 10-15 °C was achieved in this work with a 1.9 meter long duct at the tested flowrates. Further increasing the effectiveness of the dehumidifier means that the counterflowing water droplets will have a higher temperature difference with the incoming air yielding a higher rate of heat and mass transfer. One can theoretically increase the length of the dehumidifier duct to achieve a higher temperature drop, however, a larger length becomes impractical for design and laboratory scale testing. A two-stage dehumidification cycle is proposed for future investigation to increase the temperature difference between the water droplets on the strings and the incoming air. The water droplets can be formed due to the humid air as shown in this study and also, by the condensed water of the second stage falling on the strings as shown in Figure 34. This setup could increase the water beads on the strings and increase the temperature difference with the air. By utilizing strings with great water bead formation and sliding this design could potentially solve the limitations discovered in this study.

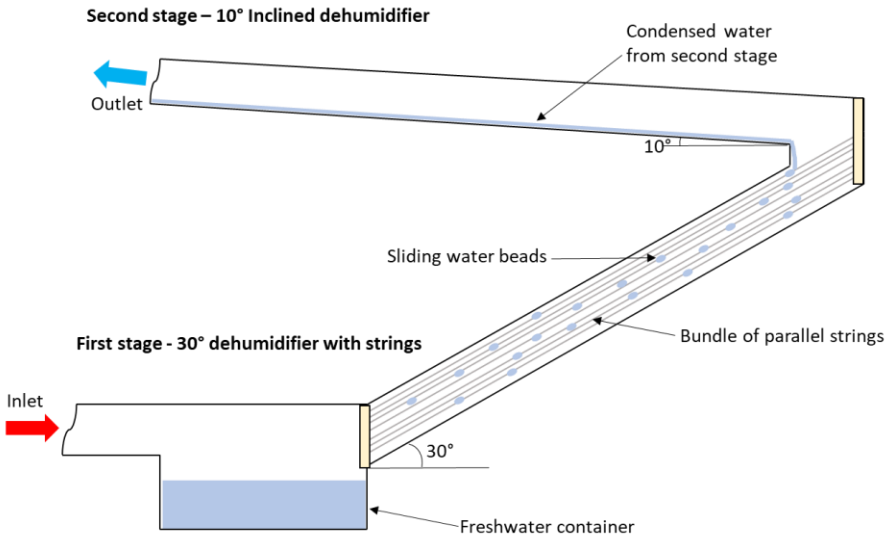

Figure 36: Proposed two-stage string-enhanced dehumidifier.

REFERENCES

[1] M. M. Mekonnen, A. Y. Hoekstra, Four billion people facing severe water scarcity. Sci. Adv. 2, e1500323 (2016).

[2] Ridoutt, Bradley G., and Stephan Pfister. "A revised approach to water footprinting to make transparent the impacts of consumption and production on global freshwater scarcity." Global Environmental Change 20.1 (2010).

[3] Zhou, Dong, et al. "Development of lower cost seawater desalination processes using nanofiltration technologies—A review." Desalination 376 (2015): 109-116

[4] Homaeigohar, Shahin, and Mady Elbahri. "Graphene membranes for water desalination." NPG Asia Materials 9.8 (2017): e427-e427.

[5] Li, Zhaohao, et al. "Water vapor capture using microporous ceramic membrane." Desalination 482 (2020)

[6] Fessehaye, Mussie, et al. "Fog-water collection for community use." Renewable and Sustainable Energy Reviews 29 (2014): 52-62.

[7] I. Shiklomanov, Water in Crisis: A Guide to the World's Freshwater Resources, Oxford University Press, New York, 1993.

[8] S. Mustafa, R. Shapawi, Aquaculture Ecosystems: Adaptability and Sustainability, 1st ed., Wiley-Blackwell, 2015.

[9] Amy, Gary, et al. "Membrane-based seawater desalination: Present and future prospects." Desalination 401 (2017): 16-21.

[10] Elmaadawy, Khaled, et al. "Optimal sizing and techno-enviro-economic feasibility assessment of large-scale reverse osmosis desalination powered with hybrid renewable energy sources." Energy Conversion and Management 224 (2020): 113377.

[11] Giwa, Adewale, et al. "Recent advances in humidification dehumidification (HDH) desalination processes: Improved designs and productivity." Renewable and Sustainable Energy Reviews 57 (2016): 929-944.

[12] D.D.W. Rufuss, S. Iniyan, L. Suganthi, P.A. Davies, Solar stills: a comprehensive review of designs, performance and material advances, Renew. Sust. Energ. Rev. 63 (2016) 464–496

[13] Giwa, Adewale, Hassan Fath, and Shadi W. Hasan. "Humidification–dehumidification desalination process driven by photovoltaic thermal energy recovery (PV-HDH) for small-scale sustainable water and power production." Desalination 377 (2016): 163-171.

[14] Al-Hallaj, Said, et al. "Solar desalination with humidification–dehumidification cycle: Review of economics." Desalination 195.1-3 (2006): 169-186.

[15] Abdelmoez, Wael, Mohamed S. Mahmoud, and Taha E. Farrag. "Water desalination using humidification/dehumidification (HDH) technique powered by solar energy: a detailed review." Desalination and Water Treatment 52.25-27 (2014): 4622-4640.

[16] Giwa, Adewale, et al. "Recent advances in humidification dehumidification (HDH) desalination processes: Improved designs and productivity." Renewable and Sustainable Energy Reviews 57 (2016)

[17] Narayan, G. Prakash, et al. "The potential of solar-driven humidification–dehumidification desalination for small-scale decentralized water production." Renewable and sustainable energy reviews 14.4 (2010): 1187-1201.

[18] A.A. ElDifrawi, C.F. Blazek, B.D. Yudow, US4363703 Thermal Gradient. Humidification-Dehumidification Desalination System, (1982).

[19] W.E. Sear, US4172767 Water Purification System, (1979).

[20] B.W. Hanning, US4187151 Apparatus for Producing Sweet Water, (1980).

[21] Yang, Yingchen. "Pressure effect on an ocean-based humidification-dehumidification desalination process." Desalination 468 (2019): 114056.

[22] Yang, Yingchen. "Desalination device." U.S. Patent Application No. 16/711,546.

[23] Fath, Hassan ES, et al. "PV and thermally driven small-scale, stand-alone solar desalination systems with very low maintenance needs." Desalination 225.1-3 (2008): 58-69.

[24] Santosh, R., et al. "Technological advancements in solar energy driven humidification-dehumidification desalination systems-A review." Journal of Cleaner Production 207 (2019)

[25] Srithar, K., and T. Rajaseenivasan. "Recent fresh water augmentation techniques in solar still and HDH desalination–A review." Renewable and Sustainable Energy Reviews 82 (2018): 629-644.

[26] Lienhard, John H. "Humidification-dehumidification desalination." Desalination: Water from Water, edited by Jane Kucera, Scrivener Publishing (2019): 387-446.

[27] K. M. Chehayeb, G. P. Narayan, S. M. Zubair, J. H. Lienhard V, Thermodynamic balancing of a fixed-size two-stage humidification dehumidification desalination system. Desalination 369, 125–139 (2015).

[28] Qasem, Naef AA, M. A. Ahmed, and Syed M. Zubair. "The impact of thermodynamic balancing on performance of a desiccant-based humidification-dehumidification system to harvest freshwater from atmospheric air." Energy Conversion and Management 199 (2019): 112011.

[29] Chafik, Efat. "Design of plants for solar desalination using the multi-stage heating/humidifying technique." Desalination 168 (2004): 55-71.

[30] Chafik, Efat. "A new type of seawater desalination plants using solar energy." Desalination 156.1-3 (2003): 333-348.

[31] Müller-Holst, Hendrik, et al. "Solar thermal seawater desalination systems for decentralised use." Renewable Energy 14.1-4 (1998): 311-318.

[32] Farid, M. M., et al. "Solar desalination with a humidification-dehumidification cycle: mathematical modeling of the unit." Desalination 151.2 (2003): 153-164.

[33] Nawayseh, Naser Kh, et al. "Solar desalination based on humidification process—I. Evaluating the heat and mass transfer coefficients." Energy conversion and management 40.13 (1999): 1423-1439.

[34] Tow, Emily W. "Experiments and modeling of bubble column dehumidifier performance." International journal of thermal sciences 80 (2014)

[35] Sadeghpour, A., et al. "Water vapor capturing using an array of traveling liquid beads for desalination and water treatment." Science advances 5.4 (2019): eaav7662.

[36] Zhao, Yunsheng, et al. "Experimental research on four-stage cross flow humidification dehumidification (HDH) solar desalination system with direct contact dehumidifiers." Desalination 467 (2019): 147-157.

[37] Niroomand, Nayereh, Mohammad Zamen, and Majid Amidpour. "Theoretical investigation of using a direct contact dehumidifier in humidification–dehumidification desalination unit based on an open air cycle." Desalination and Water Treatment 54.2 (2015): 305-315.

[38] Lawal, Dahiru U., et al. "Performance assessment of a cross-flow packed-bed humidification–dehumidification (HDH) desalination system–the effect of mass extraction." Desalin. Water Treat. 104 (2018): 28-37.

[39] Chinju, Hirofumi, Kazunori Uchiyama, and Yasuhiko H. Mori. "“String-of-beads” flow of liquids on vertical wires for gas absorption." AIChE journal 46.5 (2000): 937-945.

[40] Letan, Ruth, and Ephraim Kehat. "The mechanics of a spray column." AIChE Journal 13.3 (1967): 443-449.

[41] Nozaki, Takashi, Nobufuji Kaji, and Yasuhiko H. Mori. "Heat Transfer to a Liquid Flowing Down Vertical Wires Hanging in a Hot Gas Stream: an Experimental Study of a New Means of Thermal Energy Recovery." International Heat Transfer Conference Digital Library. Begel House Inc., 1998.

[42] Zeng, Zezhi, Abolfazl Sadeghpour, and Y. Sungtaek Ju. "Thermohydraulic characteristics of a multi-string direct-contact heat exchanger." International Journal of Heat and Mass Transfer 126 (2018)

[43] Hattori, Kenji, Mitsukuni Ishikawa, and Yasuhiko H. Mori. "Strings of liquid beads for gas-liquid contact operations." AIChE journal 40.12 (1994): 1983-1992.

[44] Park, Kyoo-Chul, et al. "Condensation on slippery asymmetric bumps." Nature 531.7592 (2016): 78-82.

[45] Zeng, Zezhi. Interfacial heat and mass transfer of liquid films flowing down strings against counterflowing gas streams. Diss. UCLA, 2019.

[46] Klös, Gunnar. Time evolution of the size distribution of droplets on a string. Diss. Georg-August-Universität Göttingen, 2013.

[47] Guo, L., and G. H. Tang. "Dropwise condensation on bioinspired hydrophilic-slippery surface." RSC advances 8.69 (2018): 39341-39351.

[48] Edalatpour, M., et al. "Managing water on heat transfer surfaces: A critical review of techniques to modify surface wettability for applications with condensation or evaporation." Applied Energy 222 (2018): 967-992.

[49] Miljkovic, Nenad, and Evelyn N. Wang. "Condensation heat transfer on superhydrophobic surfaces." MRS bulletin 38.5 (2013): 397-406.

[50] Moradi, Mostafa, Seyed Farshid Chini, and Mohammad Hassan Rahimian. "Vibration-enhanced condensation heat transfer on superhydrophobic surfaces: An experimental study." AIP Advances 10.9 (2020): 095123.

[51] Chavan, Shreyas, et al. "Heat transfer through a condensate droplet on hydrophobic and nanostructured superhydrophobic surfaces." Langmuir 32.31 (2016): 7774-7787.

[52] Khatir, Zinedine, et al. "Dropwise condensation heat transfer process optimisation on superhydrophobic surfaces using a multi-disciplinary approach." Applied Thermal Engineering 106 (2016): 1337-1344.

[53] Agarwala, Mukesh, et al. "Direct selective laser sintering of metals." Rapid Prototyping Journal (1995).

[54] Maitra, Tanmoy, et al. "Hierarchically nanotextured surfaces maintaining superhydrophobicity under severely adverse conditions." Nanoscale 6.15 (2014): 8710-8719.

[55] Comanns, Philipp, et al. "Moisture harvesting and water transport through specialized micro-structures on the integument of lizards." Beilstein journal of nanotechnology 2.1 (2011): 204-214.

[56] Zheng, Yongmei, et al. "Directional water collection on wetted spider silk." Nature 463.7281 (2010): 640-643.

[57] Hong, Daewha, et al. "Water-collecting capability of radial-wettability gradient surfaces generated by controlled surface reactions." Langmuir 26.19 (2010): 15080-15083.

[58] Wu, Huaping, et al. "Smart design of wettability-patterned gradients on substrate-independent coated surfaces to control unidirectional spreading of droplets." Soft Matter 13.16 (2017): 2995-3002.

[59] Zeng, Xinjuan, et al. "Inspired by stenocara beetles: from water collection to high-efficiency water-in-oil emulsion separation." ACS nano 11.1 (2017): 760-769.

[60] Ishii, Daisuke, Hiroshi Yabu, and Masatsugu Shimomura. "Novel biomimetic surface based on a self-organized metal− polymer hybrid structure." Chemistry of Materials 21.9 (2009): 1799-1801.

[61] Mondal, Bikash, et al. "Design and fabrication of a hybrid superhydrophobic–hydrophilic surface that exhibits stable dropwise condensation." ACS applied materials & interfaces 7.42 (2015): 23575-23588.

[62] Miyatake, O., and H. Iwashita. "Laminar-flow heat transfer to a fluid flowing axially between cylinders with a uniform surface temperature." International journal of heat and mass transfer 33.3 (1990): 417-425.

[63] Sparrow, E. M., and A. L. Loeffler Jr. "Longitudinal laminar flow between cylinders arranged in regular array." AIChE Journal 5.3 (1959): 325-330.

[64] Boukhriss, M., K. Zhani, and R. Ghribi. "Study of thermophysical properties of a solar desalination system using solar energy." Desalination and Water Treatment 51.4-6 (2013): 1290-1295.

[65] Ji, Xiaoyan. Thermodynamic properties of humid air and their application in advanced power generation cycles. Vol. 68. No. 01. 2006.

[66] Lienhard, J. H. IV, and Lienhard, J. H. V, A Heat Transfer Textbook, 4th ed., Dover Publications,Mineola, NY, 2011.

[67] Zhang, Yin, et al. "Experimental study of a humidification-dehumidification desalination system with heat pump unit." Desalination 442 (2018): 108-117.

[68] Prakash Narayan, G., et al. "Energy effectiveness of simultaneous heat and mass exchange devices." Front Heat Mass Transfer 1.2 (2010).

[69] Kazi, S. N., G. G. Duffy, and Xiao Dong Chen. "Fouling and fouling mitigation on heated metal surfaces." Desalination 288 (2012): 126-134.

[70] S. N. Kazi, K. H. Teng, M. S. Zakaria, E. Sadeghinezhad, and M. A. Bakar, “Study of mineral fouling mitigation on heat exchanger surface,” Desalination, vol. 367, pp. 248–254, Jul. 2015

[71] M¨uller-Steinhagen, H., Verschmutzung von W¨armeu ¨bertragung im U¨ bergargsbereich zwischen laminarer und turbulenter Rohrstr¨omung, Forschung im Ingenieure (Association of German Engineers), VDI-Gesellschaft Verfahrenstechnik und Chemieingenieurwese (GVC), 10th (German) ed., Springer-Verlag, Berlin, Germany, chapter Od, 2006.

[72] White, Frank M., and Joseph Majdalani. Viscous fluid flow. Vol. 3. New York: McGraw-Hill, 2006.

[73] Duarte, Juliana P., and Michael L. Corradini. "Hydraulic and heated equivalent diameters used in heat transfer correlations." Nuclear Technology 201.1 (2018): 99-102.

APPENDIX

APPENDIX

Table 4: State of the art equipment and software

Description	Purpose	Results Obtained
Dwyer liquid manometer	Pressure measurements	Velocity pressure and static pressure measurements within 5% accuracy
Compact USB Temperature and Relative Humidity Data Logger	Temperature and humidity measurements	Temperature readings with ±0.5°C (±1°F) accuracy and humidity readings with ±0.1°C (±0.1°F) accuracy
Caliper	Measuring distance	Distance measurements with a graduation of 0.001 in
Humidifier	Humid air production	Approximately 100% RH air at constant flow rate
Liquid in glass thermometer	Temperature reading	Real time continues temperature readings inside systems with a 1°C range
High precision electronic balance	Weigh produced water	Weight of water produced in grams with 0.01 g accuracy
Siemens NX	3-D design	Design of humidifier and dehumidifier to produce machining drawings

Table 4, cont.

Microsoft Excel	For calculations	Equations were used in excel to calculate the properties of air at various conditions
Microsoft Word	Organization of Thesis/Literature Review	Used to write thesis paper with appropriate formatting
Microsoft PowerPoint	Organization and creation of figures for thesis	Figures used in this study were created using Microsoft PowerPoint

BIOGRAPHICAL SKETCH

Josue Perez, ppjosue14@gmail.com, was born in Ameca, Jal., Mexico. He completed a Bachelor of Science in Mechanical Engineering at the University of Texas Rio Grande Valley in May 2020. During his undergraduate career he was introduce to the humidification-dehumidification (HDH) technology and worked on the design and testing of a mechanical air heater for this system. In the fall of 2020, he was accepted to the University of Texas Rio Grande Valley Mechanical Engineering Graduate Program, where he began working as a Graduate Research Assistant for Dr. Yingchen Yang. During his time, he continued on his passion for the HDH technology by focusing on the development and testing of a dehumidifier using parallel strings. He completed and defended his thesis and attained his Master's degree in May 2022.